EUKARYOTIC CELL, Apr. 2007, p. 693–709 Vol. 6, No. 4
1535-9778/07/$08.00+0 doi:10.1128/EC.00341-06

A 368-Base-Pair *cis*-Acting *HWP1* Promoter Region, HCR, of *Candida albicans* Confers Hypha-Specific Gene Regulation and Binds Architectural Transcription Factors Nhp6 and Gcf1p▽

Samin Kim,[1] Michael J. Wolyniak,[1] Janet F. Staab,[2,3]† and Paula Sundstrom[1,2]*

Microbiology and Molecular Pathogenesis Program, Dartmouth Medical School, Hanover, New Hampshire[1]; The Ohio State University, Columbus, Ohio[2]; and Clinical Research Division, Fred Hutchinson Cancer Research Center, Seattle, Washington 98109[3]

Received 25 October 2006/Accepted 15 December 2006

To elucidate the molecular mechanisms controlling the expression of the hypha-specific adhesin gene *HWP1* of *Candida albicans*, its promoter was dissected and analyzed using a green fluorescent protein reporter gene. A 368-bp region, the *HWP1* control region (HCR), was critical for activation under hypha-inducing conditions and conferred developmental regulation to a heterologous *ENO1* promoter. A more distal region of the promoter served to amplify the level of promoter activation. Using gel mobility shift assays, a 249-bp subregion of HCR, HCRa, was found to bind at least four proteins from crude extracts of yeasts and hyphae with differing binding patterns dependent on cell morphology. Four proteins with DNA binding activities were identified by using sodium dodecyl sulfate-polyacrylamide gel electrophoresis after separation by anion-exchange and heparin-Sepharose chromatography. One protein with high similarity to Nhp6, an HMG1 family member in *Saccharomyces cerevisiae*, and another with weak similarity to an HMG-like condensation factor from *Physarum polycephalum* implicated changes in chromatin structure as a critical process in hypha-specific gene regulation. Proteins with strong homology to histones were also found. These studies are the first to identify proteins that bind to a DNA segment that confers developmental gene regulation in *C. albicans* and suggest a new model for hypha-specific gene regulation.

Candida albicans is an opportunistic fungal pathogen that rapidly transitions between yeast, true hyphal, and pseudohyphal growth forms in response to a number of environmental stimuli, including temperature, pH, and medium composition (15, 19, 21). Changes in the external environment of *C. albicans* are known to be accompanied by changes in the genetic expression patterns of morphology-specific transcripts, leading in turn to the activation and deactivation of genetic pathways that are believed to underlie the multiple interactions of *C. albicans* with its mammalian hosts, including the colonization and invasion of tissue and resistance to host defenses (16, 28).

The true hyphal morphology of *C. albicans* (43) is notable for its enhanced adherence in comparison to yeast forms (40), and this is reflected in the presence of hypha-specific proteins that promote the invasion of and adherence to host surfaces. One such protein, Hwp1 (hyphal wall protein 1), is a glycosylphosphatidylinositol-linked cell wall protein that is abundantly expressed when *C. albicans* is in hyphal growth mode and is absent or barely detectable in the yeast morphology (41). Hwp1 is incorporated into the cell wall at the tips of apically growing hyphae, limiting its presence to hyphal surfaces (39). Hwp1 has been shown to play a key role in the attachment of *C. albicans* to human buccal epithelial cells by forming covalent bonds through its function as a substrate for epithelial transglutaminases (40). *HWP1* gene expression is regulated at the level of mRNA. Northern blot analysis reveals abundant steady-state levels of *HWP1* mRNA during hyphal growth but not yeast growth (41). Under hypha-inducing conditions, *HWP1* mRNA becomes detectable within 15 min and increases over a period of several hours (3).

The regulation of *HWP1* expression is believed to be intimately associated with a number of protein factors that themselves play key roles in the yeast-to-hypha transition. This has been shown in a variety of studies using mutants that exhibit both aberrant yeast-hypha transitions and altered *HWP1* expression patterns. Those studies implicated the cyclic AMP signaling pathway and Efg1, a downstream transcription factor of this pathway, in both processes (4, 42). A number of additional contributors to *HWP1* expression have also been uncovered, including the activators Cph2 and Tec1 (23, 37), the repressors Tup1 and Nrg1 (6, 27), and the biofilm factor Bcr1 (30). However, little has been done to explore the regulation of hypha-specific genes like *HWP1* at the level of the promoter. It remains unclear whether the effect of these and other regulatory factors on *HWP1* expression is the result of a direct interaction with promoter sequences or is instead an indirect effect of a morphogenesis regulatory pathway.

In previous work, we found that the 1,410 bp immediately upstream of the transcription start site of *HWP1* conferred successful developmental regulation to a green fluorescent

* Corresponding author. Mailing address: Dartmouth Medical School Dartmouth Regional Technology Center, 16 Cavendish Court, Centerra Research Park, Lebanon, NH 03766. Phone: (603) 676-3350. Fax: (603) 676-3359. E-mail: Paula.Sundstrom@Dartmouth.edu.

† Present address: Division of Infectious Diseases, Oregon Health and Science University, Portland, OR 97239.

▽ Published ahead of print on 12 January 2007.

protein (GFP) reporter (39). However, additional analyses have revealed that the *HWP1* promoter extends further upstream and is more complex than previously thought, necessitating the inclusion of additional DNA in the reporter plasmid. Here, we report an extensive dissection of the *HWP1* promoter that unveiled a particular region, HCR, that is critical for activation and is able to confer developmental regulation on a heterologous promoter. Different sets of HCR/DNA binding protein interactions from crude extracts of yeast and hyphal cells were observed, four such proteins were isolated and identified, and their binding to a subregion of HCR was confirmed by the use of recombinant proteins. To our knowledge, these studies are the first to identify proteins from *C. albicans* that bind to a promoter region shown to confer developmental regulation to a hypha-specific gene. The results form the basis for a new model of hypha-specific gene regulation in *C. albicans*.

MATERIALS AND METHODS

Strains and growth conditions. A complete list of strains is shown in Table 1. *C. albicans* strains were stored at −80°C prior to use. Strain CAI4 (12) was the parent strain for the preparation of the GFP reporter strains. Selection of Ura^+ CAI4 transformants containing promoter deletion plasmids was performed on yeast nitrogen base (YNB) plates supplemented with 50 mM glucose. *C. albicans* SC5314 served as the source of crude extract preparations for *HWP1* control region a (HCRa) protein binding assays and was plated onto yeast-peptone-dextrose plates supplemented with 20 μg/ml uridine at 30°C prior to use. For GFP reporter assays, yeast strains grown for 48 h to stationary phase in liquid YNB medium at 30°C and 250 rpm were used to inoculate medium 199 (Invitrogen, Carlsbad, CA), yeast-peptone-dextrose with 10% bovine calf serum (7), or modified Lee's medium (pH 6.8) (8) at a concentration of 5×10^6 cells/ml. The cells were allowed to germinate at 37°C for 2.5 h at 100 rpm unless otherwise indicated.

Luria broth (LB) or agar was used for the growth of *Escherichia coli* strains, and RM base medium (in grams per liter: Casamino Acids, 20.0; KH_2PO_4, 3.0; NaCl, 0.5; Na_2HPO_4, 6.0; NH_4Cl, 1.0; $MgCl_2$, 0.095; pH 7.0) containing 0.2% glucose was used for protein expression experiments. *E. coli* TOP10 (Invitrogen, Carlsbad, CA) and DH5α competent cells used for cloning were grown, where appropriate, in the presence of LB plus 100 μg/ml ampicillin, 25 μg/ml kanamycin, or 50 μg/ml zeomycin for plasmid selection and maintenance.

Plasmid construction. (i) GFP reporter plasmids. Plasmid pHWP1GFP3, which contains 1,410 bp of upstream sequence from the *HWP1* transcription start site, was previously described (39). Additional *HWP1* DNA upstream of position −1410 was obtained using Lambda 1, a clone from a *C. albicans* genomic library containing *HWP1* (31). Plasmid pBSRI 1.9-16 was created by cloning an 11.9-kb Lambda 1 EcoRI fragment that overlapped the *HWP1* promoter region found in pHWP1GFP3 into pBluescript SK(−). DNA regions from position −2025 or from position −1902 to the BamHI site at position −444 were amplified by PCR using primers that engineered XhoI sites at the 5′ ends (see Table 2 for primer sequences). PCR products and pHWP1GFP3 were digested with XhoI and BamHI and ligated together to create plasmids p1902.GFP3 and pHWP1.2025GFP3.

(ii) Plasmids containing promoter deletions. External deletions upstream of position −1410 were generated using pBSRI-1.9-16 as a PCR template to amplify regions between the desired 5′ end and the native BamHI site at position −444. PCR products and pHWP1GFP3 were digested with XhoI and BamHI and incubated with T4 DNA ligase (Invitrogen, Carlsbad, CA) to create plasmids p1782, p1657, and p1535 (Table 1). External deletions downstream of position −1410 were created by using pBSBglII1.8 (39) as a template in PCR to amplify regions between the desired 5′ and 3′ ends using primers to engineer HindIII and XhoI sites on the 3′ and 5′ ends of the PCR products, respectively. These products and pHWP1GFP3 were digested with XhoI and HindIII and incubated with T4 DNA ligase to create plasmids p1242, p1209, p1153, p1063, p831, p803, p555, and p140.

Internal deletion S was created by PCR-ligation-PCR (1, 2). The *HWP1* promoter regions at positions −1902 to −1410 and −1042 to +60 were PCR amplified with a genomic DNA template using primer pairs TX1902/B1411 and T1042/H39, respectively, whereas the resultant PCR products served as a template for the second reaction with primers TX1902 and H39. The final PCR product was digested with XhoI and HindIII and cloned into pHWP1GFP3 to create pSGFP3.

Internal *HWP1* promoter deletions E, M, and K2 were cloned by amplifying the −1902 to −1657, −1410 to −1042, or −1288 to −1042 region, respectively, and engineering XhoI ends by PCR with a genomic DNA template. The resulting products were ligated into p856GFP3, which contains external deletion −555, to create plasmids pEGFP3, pK2GFP3, and pMGFP3.

To test that the activating ability of the 368-bp HCR segment was not the result of spatial effects, 376 bp of DNA from the enolase coding region was cloned into plasmid pSGFP3 to replace HCR. A unique EcoRV restriction site was placed at position −1042 in plasmid pSGFP3 using the QuikChange site-directed mutagenesis kit (Stratagene, La Jolla, CA). Primer set E15 was used to amplify the replacement DNA, adding EcoRV restriction sites to either end (Table 2). The pSGFP3 site-directed mutagenesis product and the E15 PCR product were digested with EcoRV, purified, and ligated to create plasmid pSENO1.

To test whether HCR could activate a different promoter, a basal promoter was created using pENO1GFP3 (39). A unique EcoRV site 20 bp upstream from the enolase promoter TATA box was added by site-directed mutagenesis as described above. The resulting plasmid was digested with EcoRV and XhoI to remove the activating regions of the enolase promoter and purified by gel extraction (QIAGEN, Valencia, CA). Primer set HCR was used for PCR with the genomic DNA template to generate the HCR fragment from the *HWP1* promoter with engineered XhoI and EcoRV sites. The resulting PCR product and pENO1GFP3 were digested with XhoI and EcoRV and ligated to create plasmid pEX-1.

(iii) Plasmids containing putative HCRa binding protein transcripts. A 249-bp PCR fragment encompassing positions −1410 to −1162 and named HCRa was amplified using primer set TR06 with genomic DNA as a template. The HCRa PCR product was cloned into pCR4-TOPO to create pSKD19. The *C. albicans NHP6* gene with an N-terminal His_6 tag was amplified by PCR using primers NHP-h6 Xho and NHP Spe with genomic DNA as a template. The PCR product was digested with SpeI and XhoI and ligated into pPICZαC (Invitrogen, Carlsbad, CA) with digested XbaI and XhoI sites to create pSKD306. To generate pSKD703, which was engineered to have a His_6 tag at its N terminus, His_6-Nhp6 was PCR amplified from pSKD306 using primers NHP6-h6 and NHP Spe and cloned into pBAD202/D-TOPO (Invitrogen, Carlsbad, CA).

C. albicans GCF1, *HTB1*, and *HTA1* were amplified with primer sets GCF1, HTB1, and HTA1, respectively. The resultant PCR products were cloned into the pBAD202/D-TOPO vector to generate plasmids pSKD710, pSKD721, and pSKD723 that placed sequences encoding thioredoxin and a His_6 tag on their N and C termini, respectively.

All plasmid constructs were sequenced to verify accuracy.

Strain construction. (i) Integration of pHWPGFP3 at the *HWP1* locus. To create a *C. albicans* strain with GFP at the native *HWP1* locus, pHWP1GFP3 was linearized at its unique BamHI site and transformed by the spheroplast method (20) into CAI4, creating strain HB-12. Genomic DNA was digested with BglII and probed with a fragment spanning *HWP1* promoter positions −1063 to +7 to verify low-copy integration by Southern blotting (not shown).

(ii) Integration of *HWP1* promoter deletion plasmids at the *ENO1* locus. ClaI-digested plasmid DNA from each promoter deletion construct was transformed into *C. albicans* CAI4 as described above. For each construct, multiple independent transformants were analyzed by Southern blotting as previously described (39).

(iii) Preparation of crude extracts. Crude extracts from stationary-phase yeast were prepared from cultures grown for 48 h in YNB medium supplemented with 2% glucose and 120 g/liter of appropriate nutrients. Crude extracts from hyphae and yeast were prepared as described above except that cells were incubated for 1 h. To ensure that cells were uniformly destined to become true hyphae (>95%) or budding yeast, an aliquot from each culture was incubated for 3 h, and cell morphologies were verified microscopically. Cultures were collected by centrifugation at 4,000 rpm for 20 min and resuspended in breakage buffer [180 mM Tris-HCl (pH 7.5), 350 mM $(NH_4)_2SO_4$, 10 mM $MgCl_2$, 1 mM EDTA, 10% (vol/vol) glycerol, 7 mM β-mercaptoethanol, 1× protease inhibitor cocktail, 1 mM phenylmethylsulfonyl fluoride]. The cells were disrupted by three passages through a French press (20,000 lb/in^2 [1 lb/in^2 = 6.9 kPa]) and then bead beaten at 4,200 rpm and 20 s for seven cycles. The crude extract was then centrifuged at 10,000 × *g* for 2 min to remove unbroken cells and ultracentrifuged at 150,000 × *g* for 2 h at 4°C. The recovered extracts were dialyzed against buffer A (20 mM Tris-HCl [pH 8.0], 50 mM NaCl, 10 mM $MgCl_2$, 1 mM dithiothreitol, 0.5 mM EDTA, 5% glycerol).

Analysis of crude cell extracts. (i) Anion-exchange column chromatography.

TABLE 1. Strains and plasmids

Strain or plasmid	Genotype or description	Reference or source
Strains		
SC5314	Wild type	14
CAI4	Δ*ura3*::*imm434*/Δ*ura3*::*imm434*	12
HB-12	As CAI4 but with plasmid pHWP1GFP3 integrated at the *HWP1* locus	This study
EGFP3	As CAI4 but with plasmid pENO1GFP3 integrated at the *ENO1* locus	39
−2025	As CAI4 but with plasmid p2025 integrated at the *ENO1* locus	This study
−1902	As CAI4 but with plasmid p1902 integrated at the *ENO1* locus	This study
−1782	As CAI4 but with plasmid p1782 integrated at the *ENO1* locus	This study
−1657	As CAI4 but with plasmid p1657 integrated at the *ENO1* locus	This study
−1535	As CAI4 but with plasmid p1535 integrated at the *ENO1* locus	This study
HGFP3(−1410)	As CAI4 but with plasmid pHWP1GFP3 integrated at the *ENO1* locus	39
−1366	As CAI4 but with plasmid p1366 integrated at the *ENO1* locus	This study
−1242	As CAI4 but with plasmid p1242 integrated at the *ENO1* locus	This study
−1209	As CAI4 but with plasmid p1209 integrated at the *ENO1* locus	This study
−1153	As CAI4 but with plasmid p1153 integrated at the *ENO1* locus	This study
−1063	As CAI4 but with plasmid p1063 integrated at the *ENO1* locus	This study
−831	As CAI4 but with plasmid p831 integrated at the *ENO1* locus	This study
−803	As CAI4 but with plasmid p803 integrated at the *ENO1* locus	This study
−555	As CAI4 but with plasmid p555 integrated at the *ENO1* locus	This study
−140	As CAI4 but with plasmid p140 integrated at the *ENO1* locus	This study
E	As CAI4 but with plasmid pEGFP3 integrated at the *ENO1* locus	This study
K2	As CAI4 but with plasmid pK2GFP3 integrated at the *ENO1* locus	This study
M	As CAI4 but with plasmid pMGFP3 integrated at the *ENO1* locus	This study
S	As CAI4 but with plasmid pSGFP3 integrated at the *ENO1* locus	This study
HCRENO	As CAI4 but with plasmid pEX-1 integrated at the *ENO1* locus	This study
SENO	As CAI4 but with plasmid pSENO1 integrated at the *ENO1* locus	This study
Plasmids		
pCR4-TOPO	Kan^r Amp^r *lacZ*α; maintenance of PCR products	Invitrogen, Carlsbad, CA
pPICZαC	Zeo^r; protein expression in *Pichia pastoris*	Invitrogen, Carlsbad, CA
pBAD202/D-TOPO	Kan^r; protein expression in *E. coli*	Invitrogen, Carlsbad, CA
pHWP1GFP3	pBluescript SK(−) with 1,410 bp upstream of *HWP1* driving GFP expression	39
pENO1	pBluescript SK(−) with full *ENO1* open reading frame	39
pENO1GFP3	pBluescript SK(−) with full *ENO1* promoter driving GFP expression	39
pBSRI 1.9-16	pBluescript SK(−) with 11.9-kb EcoRI *C. albicans* genomic clone encompassing *HWP1* promoter	This study
pBSBglII1.8	pBluescript SK(−) with 1.8-kb BglII *C. albicans* genomic clone encompassing *HWP1* positions −1410–+6020	39
p1902.GFP3	pBluescript SK(−) with 1,902 bp upstream of *HWP1* driving GFP expression	This study
pHWP1.2025GFP3	pBluescript SK(−) with 2,025 bp upstream of *HWP1* driving GFP expression	This study
p1782	pHWP1GFP3 with *HWP1* promoter positions −1782–+60	This study
p1657	pHWP1GFP3 with *HWP1* promoter positions −1657–+60	This study
p1535	pHWP1GFP3 with *HWP1* promoter positions −1535–+60	This study
p1366	pHWP1GFP3 with *HWP1* promoter positions −1366–+60	This study
p1242	pHWP1GFP3 with *HWP1* promoter positions −1242–+60	This study
p1209	pHWP1GFP3 with *HWP1* promoter positions −1209–+60	This study
p1153	pHWP1GFP3 with *HWP1* promoter positions −1153–+60	This study
p1063	pHWP1GFP3 with *HWP1* promoter positions −1063–+60	This study
p831	pHWP1GFP3 with *HWP1* promoter positions −831–+60	This study
p803	pHWP1GFP3 with *HWP1* promoter positions −803–+60	This study
p555	pHWP1GFP3 with *HWP1* promoter positions −555–+60	This study
p140	pHWP1GFP3 with *HWP1* promoter positions −140–+60	This study
pEGFP3	pHWP1GFP3 with *HWP1* promoter positions −1410–−1042, −555–+60	This study
pK2GFP3	pHWP1GFP3 with *HWP1* promoter positions −1288–−1042, −555–+60	This study
pMGFP3	pHWP1GFP3 with *HWP1* promoter positions −1902–−1657, −555–+60	This study
pSGFP3	pHWP1GFP3 with *HWP1* promoter positions −1902–−1410, −1042–+60	This study
pSENO1	pSGFP3 with *HWP1* promoter positions −1410–−1042 replaced with 376 bp of *ENO1* coding region	This study
pEX-1	pENO1GFP3 with *ENO1* promoter replaced by *HWP1* promoter −1410–−1042	This study
pSKD19	pCR4-TOPO with *HWP1* promoter positions −1410–−1162	This study
pSKD306	pPICZαC with N-terminal His_6-tagged *NHP6*	This study
pSKD703	pBAD202/D-TOPO with N-terminal His_6-tagged *NHP6*	This study
pSKD710	pBAD202/D-TOPO with *GCF1* without stop codon	This study
pSKD721	pBAD202/D-TOPO with *HTB1* without stop codon	This study
pSKD723	pBAD202/D-TOPO with *HTA1* without stop codon	This study

TABLE 2. Oligonucleotides[a]

Oligonucleotide	Construct(s)	Sequence (5′–3′)	Site(s) added
External deletions			
TX2025	−2025	GGCCTCGAGAATTATCGGGTGATTAATAACATGC	XhoI
TX1902	−1902	GGCCTCGAGGGTAATTATTGGAATGAACGTG	XhoI
TX1840	−1840	GCCTCGAGACTAAATAGGTAATTGTTTATTTTTAGC	XhoI
TX1782	−1782	GGCCTCGAGCTAATGATTGTGACTATTGAAAATG	XhoI
TX1657	−1657	GGCCTCGAGTGGGTCTAGTAATGTTGTGC	XhoI
TX1535	−1535	GGCCTCGAGGTAAACAAACTCCCACAACCAATCG	XhoI
X2	−1410	GGCTCGAGGATCTTTCTTTTTCATTTCCC	XhoI
T1365	−1366	CCGCTCGAGGTGGAAATAAAGCTATGATAAATG	XhoI
T1288	−1289	CCGCTCGAGTGTTGTTGTCCTCGTCTCG	XhoI
T1241	−1242	CCGCTCGAGCAAGAAATACAGGAAACCCTCC	XhoI
T1208	−1209	CCGCTCGAGTTTGGACCTTACACGCAC	XhoI
X259	−1153	GGCTCGAGGAAACATACGATATGTTATTCTTT	XhoI
X348	−1063	GGCTCGAGGGTAAGAGTTGCCTAACCATTG	XhoI
X580	−831	GGCTCGAGCCACTAATTCCATCAATAAAAT	XhoI
X608	−803	GGCTCGAGGTGTATTGTTCTCTTCAGTACATT	XhoI
X856	−555	GGCTCGAGCTCGACTAATCGACTTTACATCAA	XhoI
X1271	−140	GGCTCGAGCATAGCAACTCTTGTAAAGTC	XhoI
B425	External	GAATTCCTTGTTTTT**GGATCC**AAAG	EcoRI, **BamHI**
H39	External	GGAAGCTTATTGACGAAACTAAAAGCG	HindIII
Internal deletions			
BX1042	E, K2	GGCCTCGAGCAATGGTTAGGCAACTCTTACC	XhoI
BX1289	K2	GGCCTCGAGACGTACTTTTTAACTGTCAAACGTG	
BX1657	M	CCGCTCGAGAGCTAAGAGTTTTTTATGGCATTC	XhoI
T1042	S	GAAAATAATAGGCTAAGGTTTTTCCTGATGCG	
B1411	S	CTTTATATGCTAGCAATAAAGTCAAAGAACAAGG	
Other constructs			
E15 for		GGAGATATCGATTGACCGTATTTCTTC	EcoRV
E15 rev		GGCGATATCTTGTCGACCAAGCTAAGATT	EcoRV
HCR for		GGGCTCGAGAGATCTTTCTTTTTCATTTCCCTTAAAACCGA TCAA	XhoI
HCR rev		GGGGATATCAGATGGTTAGGCAACTCTTACCTTTTCATTTCC	EcoRV
TRO6 for		AGATCTTTCTTTTTCATTTCCCTT	
TRO6 rev		TATTATGGCAAGTTTATCCGCAAT	
NHP-h6 Xho		AAAACTCGAGATG**CATCATCATCATCATCATCAT**GCTCCAGGTGA AAGAAAGAAGTCC	XhoI, **His_6 tag**
NHP-h6		CACCATG**CATCATCATCATCATCAT**GCTCCAGG	**His_6 tag**
NHP Spe		AAAAACTAGTTAGGCGGAATTCTTTTTAGCGTATTCAGCC	SpeI
mtHMG for		CACCATGTTGAGATCATTTGTAACATCTATTAGTCC	
mtHMG rev		AAAGTCATCCTCCACTTTGTAGTTTTCC	
HTB1 for		CACCATGGCCCCAAAAGCAGAAAAGAAACCAGC	
HTB1 rev		ACTAGAAGCAGATGAGTATTTTGTGACG	
HTA1for		CACCATGTCAGGTGGTAAAGGTAAAGCAGGAACTTCC	
HTA1 rev		CAATTCTTGAGAAGCCTTAACACCACC	
ENO2 for		TTGTGGGCCAGACAACCATTTAG	
ENO2 rev		CCAAAACGTTTTGAACGGTGGTTCC	

[a] Underlining, primary engineered restriction site; boldface type, additional engineered restriction site or His, tag.

To investigate the potential differences in DNA binding activities in the three growth conditions, crude hyphal, yeast, and stationary-phase yeast extracts were loaded onto a 1-ml HiTrap Q-Sepharose Fast Flow column (strong anion) (GE Healthcare, Piscataway, NJ) according to the manufacturer's instructions. A stepwise elution of proteins was carried out using increasing concentrations of NaCl (0.2, 0.3, 0.4, 0.5, and 1.0 M) in buffer A.

(ii) Ammonium sulfate precipitation and heparin-Sepharose column chromatography. To obtain preparative amounts of DNA binding proteins for amino acid sequencing, crude extracts from stationary-phase yeasts were divided into four fractions by progressive precipitation in 25%, 50%, and 75% ammonium sulfate; the supernatant fraction from the 75% ammonium sulfate precipitation served as the fourth fraction. The pellets resulting from the 50% and 75% ammonium sulfate precipitations as well as the final supernatant fraction were dialyzed twice against buffer A. Each fraction was loaded onto a 5-ml prepacked HiTrap heparin-Sepharose column (GE Healthcare, Piscataway, NJ) prior to stepwise elution with NaCl and analysis by gel mobility shift assays on each fraction.

Further fractionation using 60% ammonium sulfate was required to identify Hbp1. The pellet and the supernatant were dialyzed against buffer A, loaded onto a 5-ml prepacked heparin-Sepharose column, equilibrated with buffer A, and eluted using a model 2110 fraction collector (Bio-Rad, Hercules, CA) with a linear NaCl gradient ranging in concentration from 0.02 to 1 M at a flow rate of 1 ml/1 min. A total of 49 fractions were collected.

Trichloroacetic acid (TCA) was used to precipitate the column fractions by adding equal volumes of 20% TCA and incubating at 4°C for 30 min. Precipitates were collected by centrifugation at 13,000 rpm for 15 min, washed with cold acetone, and dissolved in sodium dodecyl sulfate (SDS)-polyacrylamide gel electrophoresis (PAGE) loading buffer.

(iii) Protein sequencing. Protein fractions showing binding to HCRa were analyzed by conventional SDS-PAGE using 16% polyacrylamide (22). The N-terminal and internal amino acid sequences of each protein were determined by the Dartmouth College Molecular Biology Core Facility using either the Edman method or matrix-assisted laser desorption ionization mass spectrometry (MALDI-MS) (10).

(iv) Purification of recombinant proteins from *E. coli*. Plasmids pSKD703, pSKD710, pSKD721, and pSKD723 were transformed into *E. coli* strain LMG194, in which the *araC* gene is under the control of the pBAD promoter. Transformed LMG194 was grown at 37°C to an optical density at 600 nm of 0.5 and then incubated for an additional 3 h with 0.2% L-arabinose to overexpress the protein of interest. Cells were disrupted by two passages through a French press (1,000 lb/in^2 [1 lb/in^2 = 6.9 kPa]) in binding buffer (50 mM Tris-HCl [pH 8.0], 250 mM NaCl, 5 mM imidazole, 10% glycerol, 0.05% Tween 20, 1 mM phenylmethylsulfonyl fluoride) and centrifuged at 13,000 rpm for 30 min. The resultant soluble fraction was applied to a Pro-Bond resin column (Invitrogen, Carlsbad, CA) and washed with buffer containing 50 mM Tris-HCl (pH 8.0), 125 mM NaCl, 10% glycerol, and 60 mM imidazole. Fusion proteins were eluted with buffer containing increasing concentrations of imidazole, dialyzed using SnakeSkin pleated dialysis tubing (7,000-molecular-weight cutoff) (Pierce, Rockford, IL) in EKMax reaction buffer (50 mM Tris-HCl [pH 8.0], 1 mM $CaCl_2$, 0.1% [vol/vol] Tween 20) overnight, treated with 0.1 U of enterokinase (Invitrogen, Carlsbad, CA) for 16 h at 37°C to remove thioredoxin, and recovered using Pro-Bond resin.

(v) Gel mobility shift assays. Gel mobility shift assays were performed as previously described (17), with modifications. Plasmid pSKD19 was digested with EcoRI, and 1 μg of the resultant HCRa fragment was end labeled with [γ-^{33}P]ATP by T4 polynucleotide kinase (Invitrogen, Carlsbad, CA). Unlabeled HCRa and an unrelated DNA fragment from the *ENO1* gene were used for competition assays. A 382-bp segment from *ENO1* was obtained by PCR using primer set ENO2 and pENO1 as a template (39). For the assay, 0.1 ng of labeled probe was incubated with the indicated amounts of protein from fractions with 200 or 500 ng of sheared salmon sperm DNA (normal conditions) (Ambion, Austin, TX) or from crude extracts with 3 μg of sheared salmon sperm DNA (high-stringency conditions) (46). The reaction mixtures were loaded onto a nondenaturing 5% polyacrylamide gel in Tris-borate-EDTA buffer (89 mM Tris base, 89 mM boric acid, 2 mM EDTA [pH 8.0]) and analyzed by using a Storm 860 PhosphorImager (GE Healthcare, Piscataway, NJ).

Monitoring GFP levels in reporter constructs. Assessment of GFP levels was performed by using 5 ml of M199 medium prewarmed to 37°C. Over 95% of the cells in each inoculated culture were observed to produce germ tubes. After germ tube induction, cells were washed twice with ice-cold phosphate-buffered saline, resuspended in 100 μl phosphate-buffered saline, and transferred into a 96-well Cytoplate (Applied Biosystems, Foster City, CA). Levels of GFP were measured by using a Victor2 1420 multilabel counter (Perkin-Elmer, Wellesley, MA) and normalized by dividing the fluorescence emitted per 1-s exposure by the absorbance seen at an optical density at 600 nm to produce relative fluorescence units. The fluorescence of each construct was expressed as the percentage of −1902 fluorescence, which was set at 100%. Epifluorescence using a fluorescein isothiocyanate cube with 470 to 490 nm of excitation and 515 to 550 nm of emission was performed to verify uniform GFP expression throughout the population. Cells were photographed at ×400 magnification with an Olympus (Center Valley, PA) BX60 microscope and MagnaFire S99806 camera and analyzed with MagnaFire v 2.1 (Optronics, Goleta, CA) and Image-Pro Plus v4.1 (Media Cybernetics, Silver Spring, MD) software. For each construct, three independent transformants that had integrated correctly at the *ENO1* locus as assessed by Southern blotting were tested. The variation within transformants was within 20% of the average for their respective constructs. A representative strain was selected for each construct, and fluorescence values were read in triplicate.

RESULTS

GFP reporter constructs reveal the region at positions −1410 to −1042 (HCR) of the *HWP1* promoter to be critical for activation. To assess whether the previously reported developmentally regulated *HWP1* promoter construct placed at the *ENO1* locus (39) in strain HGFP3 contained all of the regulatory elements associated with the *HWP1* promoter, GFP levels from this strain were compared to those of strain HB-12 containing GFP at the endogenous *HWP1* locus (see Materials and Methods). The fluorescence of HB-12 germ tubes, which are emerging true hyphae, was clearly increased relative to the germ tubes of HGFP3, as visualized by fluorescence microscopy, indicating either that pHWP1GFP3 in strain HGFP3 did not contain the complete set of regulatory elements or that integration position effects contribute to *HWP1* promoter activation. However, the inclusion of up to 2,025 bp of *HWP1* upstream DNA led to levels of fluorescence reaching 90% of those seen in HB-12, as measured by fluorometry (Fig. 1C). Other constructs revealed that the addition of DNA from −1840 bp upstream of the transcription start site also conferred near-wild-type levels of activation at the *ENO1* locus, indicating that position effects appeared to play a minor role in the activation of the *HWP1* promoter and that promoter control was retained at the *ENO1* locus. Therefore, the *ENO1* locus could be used as an integration site for analyses of the truncated and deleted *HWP1* promoter constructs described below.

To assess the kinetics of *HWP1* activation after placement in germ tube-inducing conditions, GFP expression levels were measured using fluorometry over time. GFP was detectable in HB-12 60 min after placing cells in germ tube-inducing conditions and continued to increase over a 7-h period (Fig. 1A). At each time point, HB-12 showed activation levels that were higher than those of HGFP3; however, the kinetics of activation were similar for the two strains. Plotting the ratios of fluorescence at each time point divided by the maximum expression level at 7 h postinduction for both HGFP3 and HB-12 showed that the activation of both strains followed identical kinetics despite the noteworthy difference in their magnitudes (Fig. 1B). These results showed that the promoter sequence upstream of the −1410 region served primarily to amplify the regulatory effects downstream of position −1410.

A comparison of GFP expression levels in strains with serial truncations at the 5′ end of the *HWP1* promoter was performed to identify the regions that were most important for activation (Fig. 1C). GFP levels were recorded as the percentage of fluorescence observed in the −1902 construct over the same time period, which was set at 100%. Sequence elements necessary for the transcriptional activation of the *HWP1* promoter spanned a large region, with the most important activating regions being located between positions −1100 and −1840.

The distal activating region extended from positions −1840 to −1410 and contributed approximately 50% of the total promoter activity compared to position −1902. Incremental external deletions into the 5′ end of the promoter showed a gradual decline in activation until a sharp drop from 79% to 47% activation of position−1902 fluorescence occurred upon the removal of the 125 bp between positions −1535 and −1410. This decrease was reversed upon the removal of an additional 44 bp as shown by restoration to 81% of position −1902 fluorescence in the position −1366 construct, indicating a region conferring repression. Extending the truncations past position −1366 led to a precipitous decline in fluorescence to less than 4% of that of position −1902 for constructs with less than 1,153 bp of promoter sequence.

To further define the interior regions of the *HWP1* promoter that contribute to activation, a series of internal deletion constructs was also tested. Deletion of DNA sequences between positions −1410 and −1042 in internal deletion strain S diminished promoter activity to 8.8% of that seen in position −1902 (Fig. 1D). Replacement of this region with an equivalent amount of DNA from the *ENO1* coding region in strain SENO1 did not restore promoter activity (not shown), indicating that *HWP1* pro-

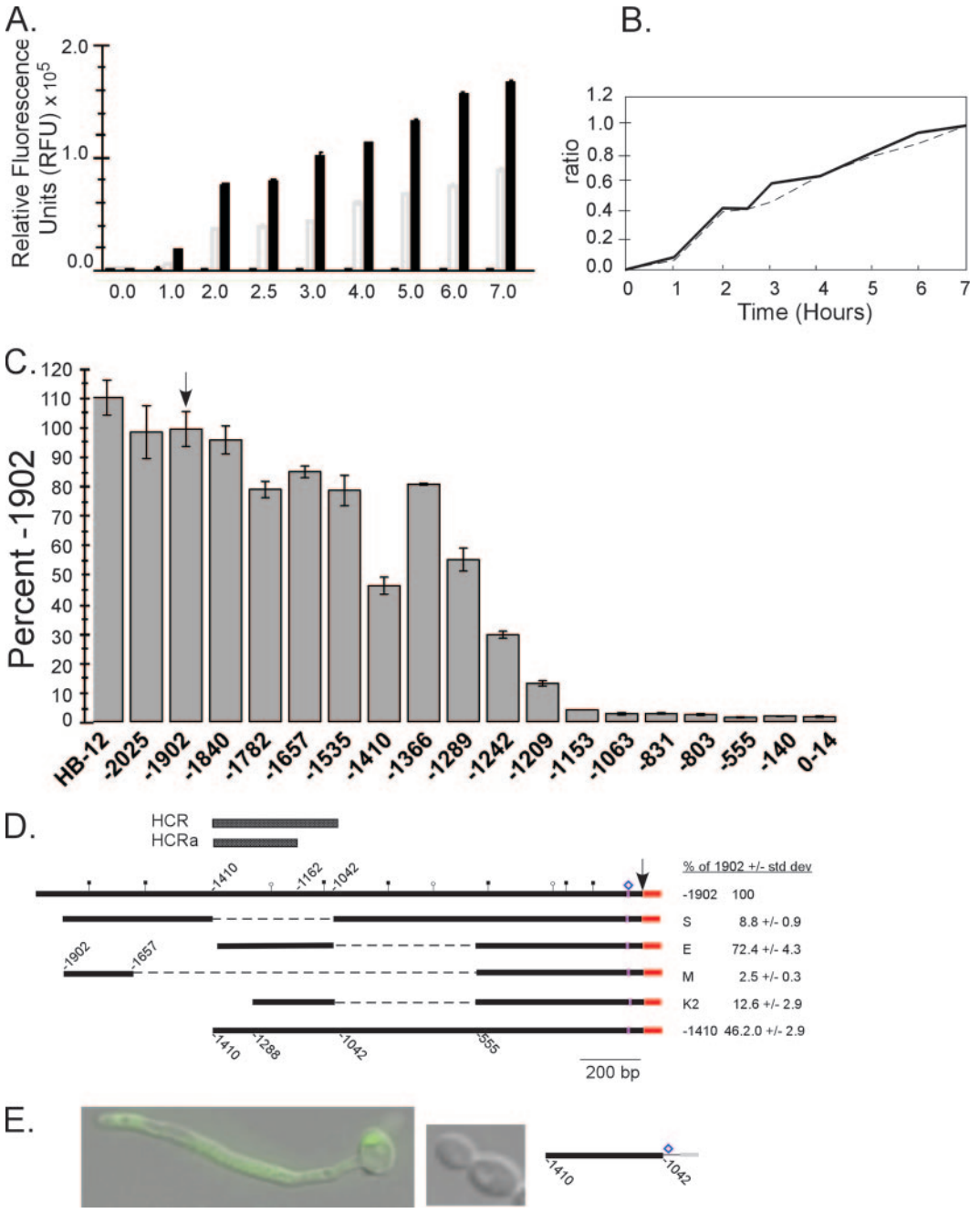

FIG. 1. Analysis of the *HWP1* promoter using GFP as a reporter. (A) Time course of GFP expression driven by various promoters including *HWP1* (strain HB-12) (black), −1410 *HWP1* (strain HGFP3) (gray), and promoterless (0GFP3) (lined). Fluorescence was quantified according to the procedures outlined in Materials and Methods. (B) Kinetics of activation of the −1410 region (dotted line) compared to the complete *HWP1* promoter (HB-12) (solid line). The values represent the ratios of the fluorescence at each time point relative to the 7-h time point. (C and D) Dissection of the *HWP1* promoter in strains containing external truncations from the 5′ end (C) and internal deletions (D). Strains were grown in M199 medium at 37°C for 2.5 h. Values represent the percent fluorescence of strain −1902, which is indicated by an arrow in C. In D, deleted DNA is indicated by a dashed line. The arrow indicates the transcription start site, and the diamond just upstream of the arrow signifies a TATA element. The locations of HCR and HCRa are shown as black bars. Putative NRE and E-box sites are indicated by open circles and black squares, respectively. (E) Developmental regulation of a heterologous promoter by HCR. HCR alone activated the truncated *ENO1* promoter, leading to GFP expression in germ tubes but not in yeast using strain HCRENO. The diamond represents the TATA box in the *ENO1* promoter.

moter activity is dependent largely on the specific sequences present within the −1410 to −1042 region and is not due simply to spatial effects. In addition, GFP fluorescence was increased from 2% to 72.4% when the promoter region between positions −1410 and −1042 was placed adjacent to a truncated construct with basal levels of activity (position −555) (Fig. 1D, construct E), indicating that sequences important for *HWP1* induction are contained within this region.

The activating ability of the region at positions −1410 to −1042 depended heavily on sequences within 200 bp down-

stream of position −1410. A construct containing the *HWP1* promoter region from positions −1288 to −1042 resulted in an activation level of only 12.6% when placed adjacent to position −555 (Fig. 1D, construct K2). This result, coupled with a comparison of the GFP fluorescence exhibited by external truncations at positions −1410 and −1366, indicate that the region of the *HWP1* promoter between positions −1410 and −1288 contains both activating and repressing activities.

In contrast to the promoter region between positions −1410 and −1042, the more distal region from positions −1902 to −1657 that appeared to confer activation ability in the truncation analysis was not sufficient to activate GFP fluorescence when placed adjacent to the truncated −555 construct with basal promoter activity (Fig. 1D, construct M). This result showed that the region from positions −1902 to −1657 serves to enhance the activating function of the region between positions −1410 and −1042.

Importantly, the region from positions −1410 to −1042 was also able to activate a heterologous promoter. Placement of this region 20 bp upstream of the TATA element of an *ENO1* promoter in strain HCRENO led to a fluorescence level of 50% of position −1902 under germ tube-inducing conditions, a level equivalent to that generated by the −1410 external deletion (Fig. 1E). The truncated *ENO1* promoter by itself failed to show GFP fluorescence (not shown), indicating that the sequences between positions −1410 and −1042 are capable of high levels of gene activation in a developmentally regulated fashion independent of other sequences in the *HWP1* promoter. Because of its ability to confer hypha-specific regulation of *HWP1*, the region from positions −1410 to −1042 was designated the HCR.

The entire *HWP1* promoter was analyzed for the presence of binding sites for Nrg1 and Efg1 (27, 42). A single Efg1 binding site (E box) from positions −1090 to −1085 and a single Nrg1 binding site (NRE) from positions −1228 to −1223 were found in HCR. E boxes were found upstream of HCR, which is suggestive of a possible role for Efg1 in the amplification of the *HWP1* promoter (Fig. 1D). Additional E boxes and NREs were also found downstream of the activating regions.

The relative levels of activation between the constructs described above were found to depend on the induction of germ tubes and were not dependent on the media used to induce germ tubes. However, the absolute level of activation was increased by 2.1-fold by the addition of 10% bovine calf serum to M199. Under yeast growth conditions, all strains showed negligible levels of *HWP1* promoter activity (not shown). Pseudohyphal forms did not activate the *HWP1* promoter to the high levels associated with germ tubes but were variably capable of producing low levels of *HWP1* promoter activity (38).

Identification of proteins from crude extracts binding to the HCRa promoter region. Given its apparent importance in the hypha-specific activation of *HWP1*, it was of interest to identify DNA binding proteins in crude *C. albicans* extracts that bound to the HCR. In addition, we wished to identify differences in the protein binding patterns in hyphal versus yeast growth forms at an early time point following hypha induction, when the mechanisms involved in promoter activation would be in progress. To this end, extracts were prepared from cells that had been placed in hypha-inducing conditions for 1 h, a period known to be early in the kinetics of activation, when *HWP1* mRNA is abundant but not yet at its peak level (3). Crude extracts were also prepared from comparable cultures incubated at 25°C for 1 h, allowing these cells to retain a yeast morphology. Crude extracts from stationary-phase yeast cultures were also included to reveal DNA binding proteins present in the absence of active growth. Henceforth, we refer to these preparations as hyphal extracts (HE), yeast extracts (YE), and stationary-phase extracts (STE).

The crude extracts were analyzed by gel mobility shifts. Experiments using the 5′ portion of the *HWP1* promoter region extending from positions −1410 to −1162, termed HCRa, showed the same DNA-protein binding pattern on nondenaturing gels as the original HCR (positions −1410 to −1042) identified in the promoter deletion analysis (data not shown). Therefore, HCRa was used in the gel mobility shift experiments described below.

Two major protein-DNA complexes that migrated slower than free HCRa were detectable in crude extracts from hyphae, yeast, and stationary-phase yeast cells under high-stringency reaction conditions (46) (see Materials and Methods). The amount of protein binding HCRa was enhanced when higher amounts of crude extract were used, suggesting a strong interaction between the two proteins and HCRa. Protein-DNA complex 2 appeared on the gel initially as two separate bands (Fig. 2A) of similar molecular weights with additional bands apparent at higher extract concentrations, suggesting the presence of a single protein with a tendency to multimerize (Fig. 2A, lanes 4, 5, and 6). The intensity of protein-DNA complex 2 appeared to be less in STE at all protein concentrations compared to those in YE and HE, suggesting that the protein present in complex 2 has decreased binding activity when the cells of origin were not actively growing. In contrast, protein-DNA complex 1 was found in HE, YE, and STE as a single shifted band across all crude extract concentrations. These results suggested that at least two distinct proteins occupy HCRa of the *HWP1* promoter with distinct binding profiles that are influenced by growth conditions.

The putative *HWP1* promoter binding proteins were specific in their binding to HCRa. Competition assays (Fig. 2B) revealed that the relative amount of the two protein-HCRa complexes observed in the above-described experiments was greatly reduced in the presence of a 200- or 50-fold molar excess of unlabeled HCRa (Fig. 2B, lanes 2 and 3) but not in the presence of a 200-fold molar excess of *ENO1* DNA (Fig. 2B lanes 4). Protein-DNA complex 1 was competed less well by unlabeled HCRa than protein-DNA complex 2, suggesting that this complex is stable. The inability of DNA to compete away either complex was consistent with the low level of activation in strain SENO1, in which HCR had been replaced with irrelevant *ENO1* DNA, and revealed that the putative HCRa binding proteins do not bind DNA in general but are specific in their interactions with HCRa.

At least four proteins appear to bind HCRa. Crude extracts were further fractionated with anion-exchange column chromatography followed by gel mobility shift assays under normal conditions in an attempt to identify proteins that exhibited differing binding activities in relation to growth conditions. The protein originally identified in protein-HCRa complex 2 (Fig. 2A) was named Hbp1, (*HWP1* control region binding protein

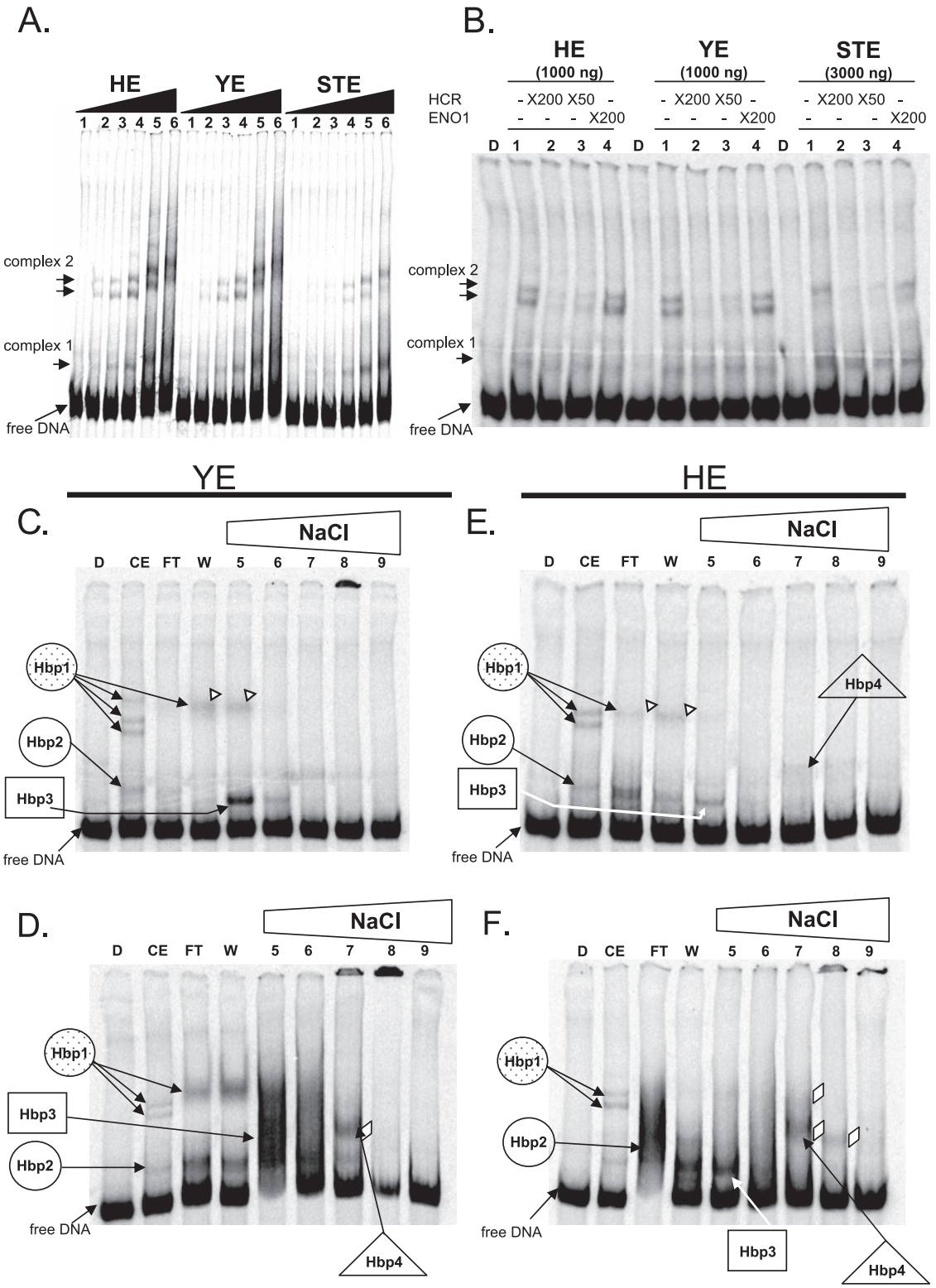

FIG. 2. Identification of HCRa-protein complexes using crude protein extracts and fractionation by anion-exchange chromatography and gel mobility shift assays performed on either a 15- by 19-cm vertical gel electrophoresis system (Life Technologies, Gaithersburg, MD) at 200 V for 2 h (A and B) or a 7- by 10-cm Mini-PROTEAN 3 cell (Bio-Rad, Hercules, CA) at 120 V for 50 min (C to F). (A) Crude extracts (HE, YE, and STE) were mixed with γ-^{33}P-labeled HCRa in the presence of 3 μg sheared salmon sperm DNA (high-stringency reaction conditions). Protein-DNA complexes 1 and 2, as well as free DNA, are indicated by arrows. Amounts of crude extract used were as follows: lane 1, 0 ng (DNA only); lane 2, 250 ng; lane 3, 500 ng; lane 4, 1,000 ng; lane 5, 3,000 ng; lane 6, 5,000 ng. (B) Competition assay in the presence of unlabeled HCRa and *ENO1* DNA. The γ-^{33}P-labeled fragment was incubated with 1,000 ng of crude extract from YE and HE and 3,000 ng from STE. Lane D, labeled probe only; lane 1, crude extract only; lanes 2 and 3, 200- and 50-fold molar excesses of unlabeled HCRa, respectively; lane 4, 200-fold molar excess of a region of *ENO1* (see Materials and Methods). (C to F) Fractions prepared from YE and HE containing 25 ng (C and E) or 250 ng (D and F) of protein were mixed with γ-^{33}P-end-labeled HCRa in the

1). The number of bands associated with Hbp1 was variable and depended on the assay conditions. When normal conditions were used with the fractions from ion-exchange chromatography, Hbp1 appeared as a single band (Fig. 2C and E).

Although Hbp1 was present in crude extracts under all growth conditions, subtle differences were seen in its behavior between YE and HE. Using the conditions for the crude extracts (Fig. 2C to F, CE lanes), Hbp1 frequently consisted of three distinct shifted bands in YE (Fig. 2C, CE lane), which is suggestive of Hbp1 monomers, dimers, and tetramers or multimers in the yeast crude extract, respectively. However, only two bands were observed in HE, which is suggestive of monomers and dimers (Fig. 2E, CE lane). Under normal conditions, the mobility of the Hbp1-HCRa complex was retarded at a rate equivalent to that of the mobility of a possible tetrameric or multimeric structure of the protein in YE compared to the putative dimeric or less multimerized form in HE (compare positions indicated by white arrowheads in Fig. 2C, lanes W and 5, and E, lanes FT and W, relative to the position of the bands in lanes labeled CE). Hbp1 also showed different elution patterns in YE and HE in that DNA binding was detected in the wash and 0.2 M NaCl fractions from YE (Fig. 2C, lanes W and 5) and in the flowthrough and wash fractions from HE (Fig. 2E, lanes FT and W). Even more striking was the finding that Hbp1 appeared to show a particularly high binding affinity for HCRa in YE, an observation that was not made with the original crude extracts using high-stringency conditions. In the assays using 250 ng of eluted protein, the Hbp1-shifted protein-DNA complex was detectable even in the flowthrough fraction in YE (Fig. 2D, lane FT). In contrast, fractions containing Hbp1 from HE showed comparatively weak binding activities (Fig. 2F, lanes FT and W). Together, these results suggest that Hbp1 may be conformationally altered depending on environmental stimuli with increased binding activity under yeast growth conditions.

Protein-HCRa complex 1 from Fig. 2A was detectable in the flowthrough and wash fractions in both YE and HE; however, the binding activity of this protein, designated Hbp2, was reduced in YE compared to HE. Gel shifts with only 25 ng protein clearly showed a complex formed by Hbp2 in the flowthrough fraction of HE, which was barely detectable in YE (Fig. 2C and E, lanes FT and W). Using 250 ng of eluted protein, the entire amount of free DNA was shifted and formed a polydispersed smear using HE that consisted of aggregates of Hbp2 alone or complexed with other proteins. In YE, most of the DNA remained unbound, and the shifted band formed a tight, rapidly migrating complex consistent with reduced binding activity in YE in comparison to HE (Fig. 2D and F, FT lanes). Overall, this suggested that Hbp2 may be active specifically under conditions of hyphal growth or may recruit other proteins during hyphal morphogenesis.

A third protein, named Hbp3, was detected and produced a shifted band that was slightly smaller than that produced by Hbp2 (Fig. 2E, compare the size of the band just above the free DNA in the FT lane [Hbp2] and lane 5 [Hbp3]) and, unlike Hbp2, was specifically eluted in the 0.2 M NaCl fraction. Hbp3 is evident in Fig. 2C by the presence of an abundant shifted band in lane 5, which is diminished in lane 6, that is not formed in the flowthrough and wash fractions. Even though Hbp3 is present in reduced amounts in HE, the elution characteristics are consistent with those from YE. The higher intensity of the band in lane 5 compared to that in lane W in Fig. 2E is consistent with optimal elution at 0.2 M NaCl. The increased abundance in YE is also seen using higher amounts of protein. Using 250 ng of eluted protein, the entire amount of free DNA was shifted, forming a polydispersed smear using YE that consisted of aggregates of Hbp3 alone or complexed with other proteins. By contrast, in HE, most of the DNA remained unbound, and the shifted band formed a tight, rapidly migrating complex consistent with less binding activity (Fig. 2D and F, lanes 5).

An additional protein, Hbp4, was detectable in the 400 mM NaCl fraction using 25 ng of eluted protein from HE (Fig. 2E, lane 7) but not from YE (Fig. 2C, lane 7). When 250 ng of eluted protein was used, Hbp4 was detectable in both the 400 and 500 mM NaCl fractions in HE (Fig. 2F, lanes 7 and 8) but only in the 400 mM NaCl fraction in YE (Fig. 2D, lane 7). In addition, multimeric forms of Hbp4 were observed in the 400 mM NaCl fraction in HE (Fig. 2F, lane 7). It is important that the binding activities of Hbp3 and Hbp4 were not confined exclusively to a single growth form. Although Hbp3 was notably more active in YE compared to HE, it was not completely absent from the latter. Likewise, Hbp4 was expressed predominantly in HE but was present at low levels in YE as well. We also observed the presence of protein-DNA complexes that failed to migrate during electrophoresis located immediately below the wells in both YE (Fig. 2C, lane 8, and D, lanes 7 and 8) and HE (Fig. 2F, lanes 8 and 9). Taken together, these results show that HCRa binds several *C. albicans* proteins and that their binding activities appear to be strongly influenced by growth conditions.

Purification and identification of HCRa binding proteins. To obtain preparative amounts of Hbp1 and Hbp2, crude extracts from stationary-phase cultures were prepared and fractionated by ammonium sulfate precipitation. The proteins of interest were observed to retain their binding activities in fractions from stepwise ammonium sulfate precipitation (Fig. 3A). Hbp1 was detectable mainly in the 25% and 50% ammonium sulfate fractions, whereas Hbp2 was found in all of the ammonium sulfate precipitated fractions as well as in the supernatant fraction. In subsequent heparin-Sepharose column chromatography from these precipitations, the protein components responsible for the different complexes with HCRa were eluted with 0.5 M and 1 M NaCl from the 50% and 75% ammonium sulfate and supernatant fractions (Fig. 3B, C, and D). The fractions in which protein-DNA complexes could be seen in gel

presence of 200 ng (C and E) or 500 ng (D and F) sheared salmon sperm DNA except for assays in lanes labeled CE, which were performed under high-stringency conditions as in A and B. The positions of the free DNA and four protein-DNA complexes (Hbp1 to Hbp4) are indicated by arrows. White arrowheads (C and E) and diamonds (F) represent Hbp1 and Hbp4, respectively. See Results for a complete explanation. Lane D, DNA only; CE, crude extract; FT, flowthrough; W, wash; lane 5, 0.2 M NaCl; lane 6, 0.3 M; lane 7, 0.4 M; lane 8, 0.5 M; lane 9, 1.0 M.

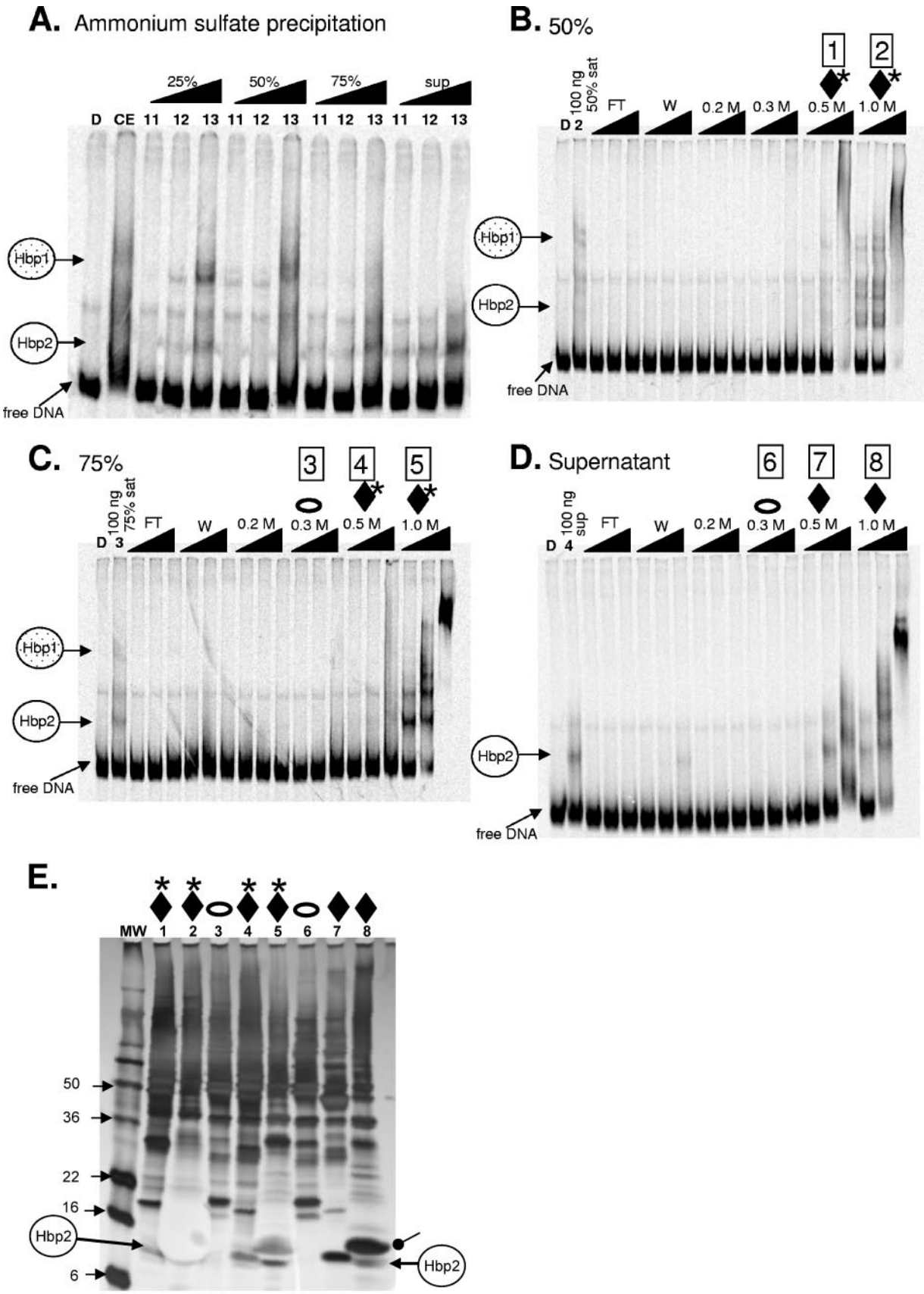

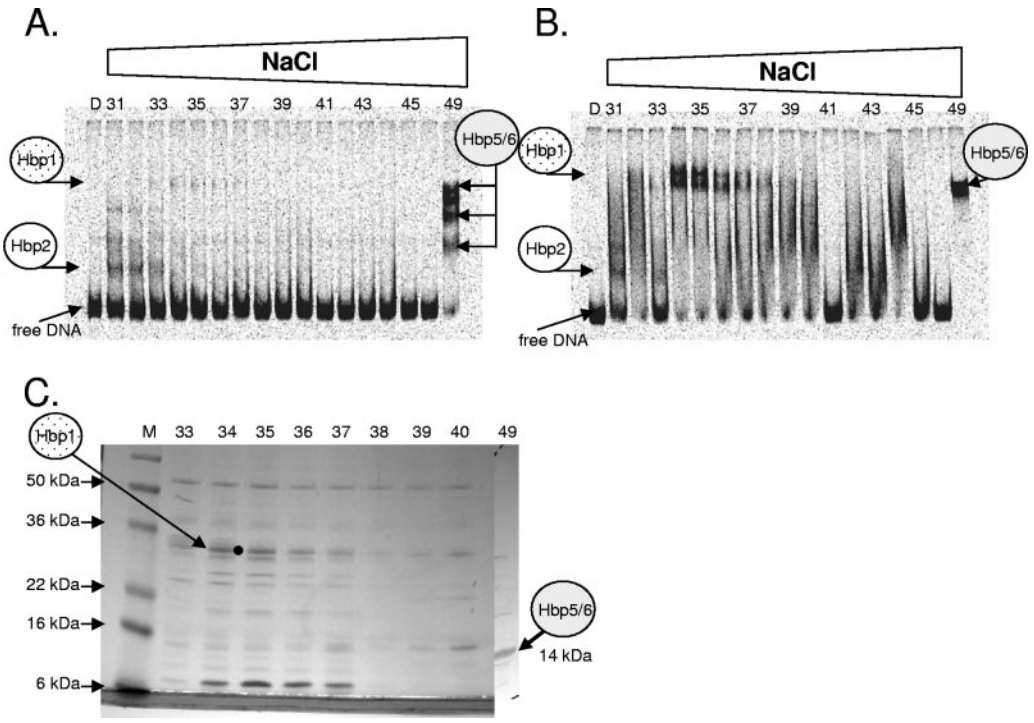

FIG. 4. Isolation of Hbp1. STE was precipitated with 60% ammonium sulfate and further fractionated with heparin-Sepharose chromatography using a 20 to 1,000 mM NaCl gradient. γ-^{33}P-labeled HCRa (0.1 ng) was mixed with 50 ng of each fraction in the presence of 200 ng sheared salmon sperm DNA (A) or 250 ng of each fraction in the presence of 500 ng of sheared salmon sperm DNA (B). Lane D contains radiolabeled probe only. (C) Coomassie blue-stained 16% SDS-polyacrylamide gel to visualize Hbp1 (see arrow and dot next to band) and Hbp5/6. Each lane contained a 5-μg sample from the indicated fraction following TCA precipitation.

mobility shift assays were compared with those fractions that did not show the presence of DNA binding proteins. A relatively small protein of about 11 kDa was absent from fractions that did not bind HCRa DNA but was present in other fractions (Fig. 3E, compare lanes 1, 2, 4, 5, 7, and 8 with lanes 3 and 6). A band correlating with Hbp1 binding activity was not apparent.

In further attempts to identify Hbp1, crude STE was subfractionated by precipitation using 60% ammonium sulfate followed by column chromatography. The concentration of ammonium sulfate was chosen based on the presence of Hbp1 DNA binding activity in the precipitate and because of the larger amount of protein precipitated compared to lower ammonium sulfate concentrations in which lower protein yields were obtained (data not shown). Fractions 34 to 40 of this separation contained the highest levels of Hbp1 (Fig. 4A and B) and exhibited the characteristic multimers exhibited in the CE lanes in Fig. 2C to F. Further analysis revealed that those fractions that possessed shifted complexes all contained a protein of about 31 kDa (Fig. 4C) that was present in highest concentration in fraction 34 with decreasing amounts in subsequent fractions that paralleled the decrease in binding activity of Hbp1. This protein was not seen in fractions that were not shifted in previous assays (data not shown). Although the 31-kDa band was the most prominent band that was specific to the fractions that produced gel shifts, other bands that migrated faster were also detected and may also have contributed to complex 2 in crude extracts (Fig. 2A and B). Identification of these additional bands is in progress. Unexpectedly, the 49th and final fraction eluted with 1 M NaCl contained a protein that produced a shifted complex distinct from those seen with

FIG. 3. Fractionation of DNA binding proteins in STE by ammonium sulfate precipitation (A) followed by heparin-Sepharose column chromatography of each ammonium sulfate fraction (B to D). Gel mobility shift assays were performed in the presence of 500 ng sheared salmon sperm DNA (A) or with 200 ng sheared salmon sperm DNA using the heparin-Sepharose fractions from stepwise elutions with NaCl from the 50% (B), 75% (C), and supernatant (D) ammonium sulfate fractions. Lane D, DNA only; lane CE (1,000 ng), crude extract under high-stringency conditions (see Materials and Methods); FT, flowthrough fraction; W, wash fraction; lanes 2, 3, and 4, 100 ng protein from 50% and 75% ammonium sulfate saturated fractions and the supernatant fraction, respectively; lanes 11, 12, and 13, 25 ng, 100 ng, and 500 ng protein, respectively, from the indicated fractions. Fractions that were compared by SDS-PAGE in E are marked with asterisks and diamonds to indicate the presence of Hbp1 and Hbp2, respectively, and with ovals to indicate fractions that did not show binding activities for either protein. The boxed numbers correspond to the lane numbers in E that were used for separating the indicated fractions by SDS-PAGE. (E) Silver-stained 16% SDS-polyacrylamide gel of representative Hbp1- and Hbp2-containing fractions as determined by assays shown in C and D. Each lane contains 1 μg of the appropriate fraction. The location of Hbp2 is indicated. The band indicated by the black dot was later found to contain histones (Fig. 4). MW, molecular weight (in thousands).

TABLE 3. Protein sequence determined by MALDI-MS or N terminal amino acid sequencing

Originally assigned name	Protein	Amino acids[a]	Sequence coverage (%)	Predicted molecular mass (kDa)
Hbp1	Gcf1p	ATKVATTTTKKTTKKAGDSVAEFYQFPEEEKYVQENYIR	15	28
Hbp2	Nhp6	MAPGERKKSSRKKKDPDAPKRSLSAYMFFANENRDIVR AENPGISFGQVGKLLGEKWKALNSEDKLPYENKAEAD KKRYEKEKAEYAKKNSA	42	11
Hbp5	Htb1	MAPKAEKKPASKAPAEKKPAAKKTATSGTKKRSKTRKET YSSYIYKVLKQTHPDTGISQKAMSIMNSFVNDIFERIAG EASKLAAYNKKSTISAREIQTAVRLILPGELAKHAVSEG TRAVTKYSSAAN	32	14
Hbp6	Hta1	MSGGKGKAGSSEKASTSRSAKAGLTFPVGRVHRLLRKG NYAQRVGSGAPVYLTSVLEYLAAEILELAGNAARDNK KSRIIPRHLQLAIRNDEELNKLLGHVTIAQGGVLPNIHQ NLLPKKSAKGKASQEL	17	14

[a] The amino acids determined by sequencing are underlined.

Hbp1 and Hbp2 on nondenaturing gels (Fig. 4A and B, fraction 49). A band corresponding to a mass of approximately 14 kDa, which was ultimately shown to contain two proteins (see below), was seen in this fraction (Fig. 4C, fraction 49). These proteins were named Hbp5 and Hbp6.

Following trypsin digestion and mass spectroscopic analysis, a peptide from Hbp2 was determined to contain the sequence APGERKKSSR (Table 3), a sequence which was identical to the *C. albicans* nonhistone protein 6 (Nhp6). A BLAST analysis of this sequence revealed that the Nhp6 protein has a predicted mass of 10,508 Da, which matched the molecular weight of the band corresponding to Hbp2 in Fig. 3E, and sequence similarity to *Saccharomyces cerevisiae* Nhp6A and Nhp6B, both of which have been shown to bind and bend DNA (18) and to encode high-mobility-group (HMG)-like proteins that influence cell and colony morphology (11). The isolated peptides were subjected to trypsin digestion and found by MALDI-MS to have 42% cumulative coverage of the Nhp6 protein (Table 3).

N-terminal amino acid sequencing of Hbp1 revealed a sequence of ATKVATTTTK. The sequence of three additional Hbp1 peptides was determined following trypsin digestion and mass spectroscopic analysis. The corresponding protein has a predicted mass of 28,355 Da, which matched the molecular

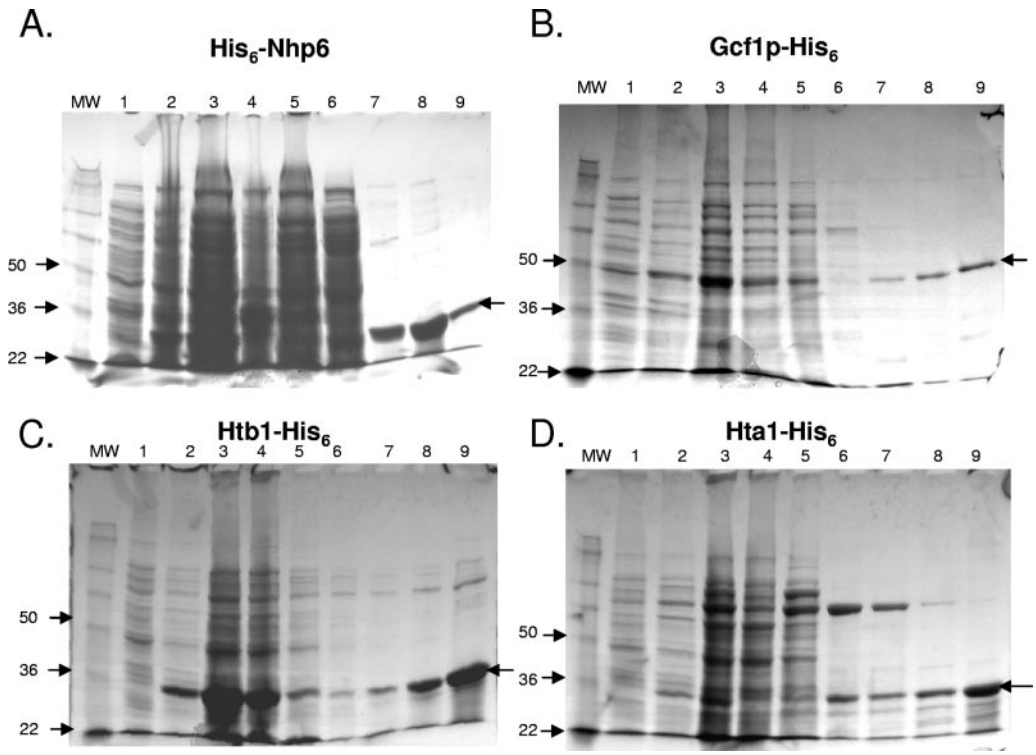

FIG. 5. Overexpression of recombinant putative HCRa binding proteins. Extracts of strains producing His_6-Nhp6 (A), Gcf1p-His_6 (B), Htb1-His_6 (C), and Hta1-His_6 (D) were analyzed on a Coomassie blue-stained SDS gel. Lane 1, preinduction; lane 2, postinduction; lane 3, soluble fraction; lane 4, insoluble fraction; lane 5, flowthrough; lane 6, wash; lane 7, 0.1 M imidazole elution; lane 8, 0.2 mM imidazole; lane 9, 0.5 M imidazole. MW, molecular weight (in thousands).

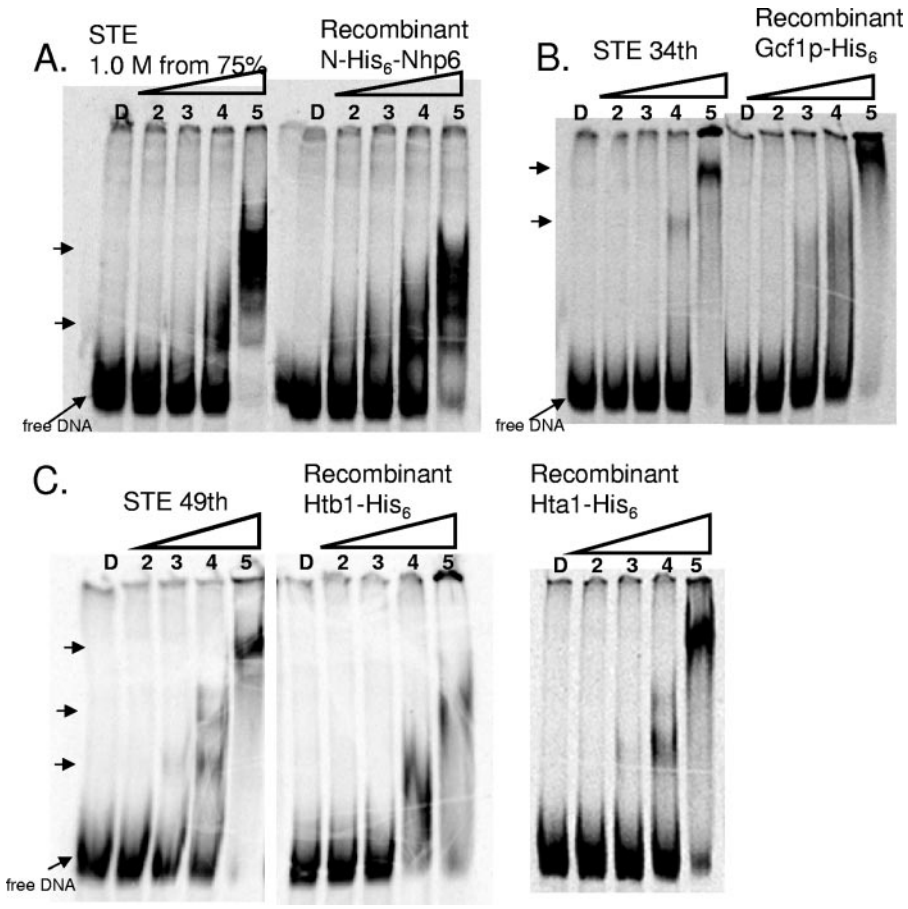

FIG. 6. Comparison of recombinant proteins Hbp1, Hbp2, Hbp5, and Hbp6 with proteins from STE to bind to HCRa. (A) Eluate from the 1.0 M NaCl–75% ammonium sulfate precipitation fraction shown in Fig. 3C compared to purified N-His_6-Nhp6. (B) Fraction 34 shown in Fig. 4A to C compared to purified Gcf1p-His_6. (C) Fraction 49 shown in Fig. 4A to C compared to purified Hta1- and Htb1-His_6. Protein-HCRa complexes and free DNA are indicated by arrows. Protein amounts used were as follows: lane 1, 0 ng; lane 2, 2 ng; lane 3, 10 ng; lane 4, 50 ng; lane 5, 250 ng.

weight of the band corresponding to Hbp1 in Fig. 4C, and shows similarity to an HMG-like protein, Glom, from *Physarum polycephalum*, that functions as a mitochondrial DNA condensation factor and is rich in lysine residues (21.7%) (36). Because of the similarities to Glom in amino acid sequence, the high content of lysine residues (19.0%), and the presence of an HMG box located near the C terminus, Hbp1 was named Glom-like condensation factor 1 (Gcf1).

Sequence analysis of Hbp5 and Hbp6 revealed internal peptides with identities to two predicted *C. albicans* histone proteins, Hta1 and Htb1. The internal peptides showed 17% coverage of Hta1 and 32% coverage of Htb1 (Table 3). Hta1 and Htb1 have predicted masses of 13,861 Da and 13,988 Da, which matched their observed masses on SDS-PAGE gels. A BLAST analysis also revealed a strong similarity to *S. cerevisiae* histones Hta1 and Htb1, subunits of the nucleosome (29).

Two HMG proteins and histones Htb1 and Hta1 bind to HCRa at the *HWP1* promoter. The genes *NHP6*, *GCF1*, *HTB1*, and *HTA1* were each cloned into plasmid pBAD202/D-TOPO and transformed into *E. coli* strain LMG194 to facilitate the overexpression of fusions between the *C. albicans* proteins and thioredoxin and His_6 tags following induction with 0.2% L-arabinose (see Materials and Methods). Major bands with mobilities of 25 kDa (Nhp6), 45 kDa (Gcf1p), and 28 kDa (Hta1 and Htb1), which were the expected sizes of each fusion protein of interest when factoring in the 11.7-kDa thioredoxin and 2-kDa His_6 tags, were found in crude extracts from *E. coli* LMG194 induced with arabinose and carrying the appropriate plasmids (Fig. 5). These results indicated that the overproduced proteins were the expected fusion proteins of interest.

The purified His_6-Nhp6, Gcf1p-His_6, Htb1-His_6, and Hta1-His_6 proteins were tested for their ability to bind HCRa by gel mobility shift assays. The fusion proteins bound efficiently to the DNA fragment carrying HCRa and showed increased binding abilities upon increasing the protein concentration (Fig. 6). Gel mobility shift assays using the recombinant proteins mirrored those seen using extracts from stationary-phase *C. albicans* cells containing the corresponding endogenous proteins, especially for the most rapidly migrating shifted bands, which are indicative of monomeric protein-DNA complexes. The differing appearances of shifted bands formed by the recombinant proteins and the proteins in STE (Fig. 6B and C, compare lane 5 in each) are most likely the result of the presence of additional unidentified proteins in STE that influence the multimerization properties of the proteins in the shifted bands. Competition experiments similar to those shown in Fig. 2B

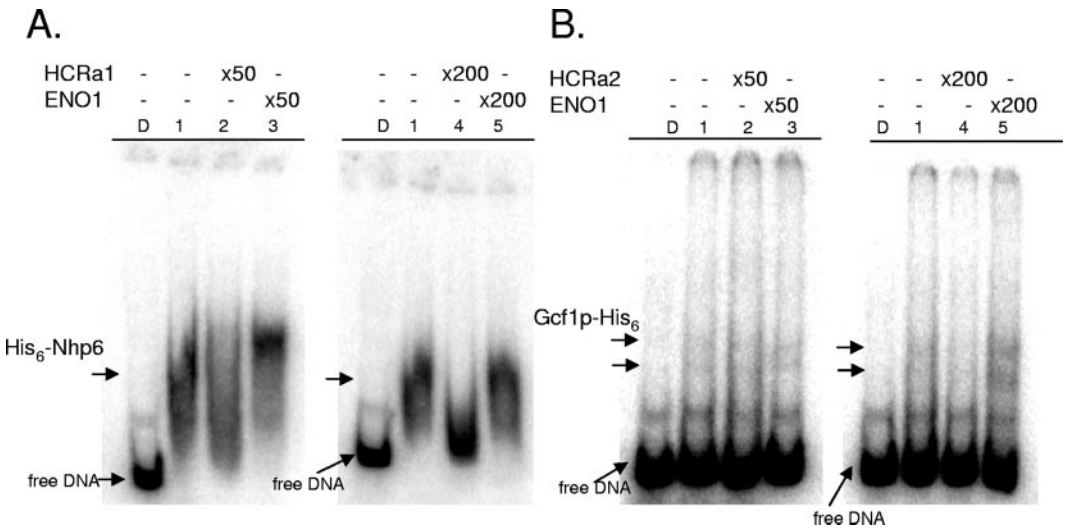

FIG. 7. Competition assay in the presence of 50- and 200-fold molar excesses of unlabeled DNA fragments from HCR and *ENO1*. Recombinant proteins (100 ng) His_6-Nhp6 (A) and Gcf1p-His_6 (B) were incubated with γ-^{33}P-labeled subregions of HCRa designated HCRa1 and HCRa2 (positions −1410 to −1249 and positions −1322 to −1162, respectively) or with a 160-bp region of *ENO1* (positions +1250 to +1405) in the presence of 1,000 ng salmon sperm DNA. Lane D, probe only; lane 1, protein only; lanes 2 and 4, 50- and 200-fold unlabeled DNA from HCR; lanes 3 and 5, 50- and 200-fold *ENO1* DNA.

using His_6-Nhp6, and Gcf1p-His_6 showed that, like the proteins in native extracts, the recombinant proteins were not competed away by irrelevant DNA (Fig. 7).

DISCUSSION

The regulation of morphology-specific gene expression is a poorly understood process that is critical for the ability of *C. albicans* to adapt to and invade human hosts. The findings in this work have identified an unusually long *HWP1* promoter and have elucidated a critical *cis*-acting region, HCR, which independently confers developmental regulation to a heterologous promoter. The discovery of a highly conserved protein, Nhp6, as well as a novel architectural HMG protein, Gcf1p, that bind specifically to this region suggests that chromatin structure may play a key role in the developmental regulation of hypha-specific genes. These findings are in agreement with work from other laboratories showing that that the Swi/Snf complex is required for *HWP1* gene expression and morphogenesis (26) and that histone modification is important for normal morphogenesis (33).

The activity of the *HWP1* promoter for external deletion constructs between positions −1410 and −1042 correlated roughly with length and did not appear to be dependent on discrete activation motifs that typically form the basis of regulatory elements. Instead, a centrally located 368-bp critical region, HCR, was found, which conferred developmental regulation independently of other *HWP1* promoter DNA and was characterized by having both activating and repressing activities located in close proximity to each other. Deletions into the 5′ end of HCR resulted in the loss of activating properties, whereas internal deletions into the 3′ region showed mixed results (not shown). The activating ability of HCR might have been enhanced if additional 5′ sequences had been included based on the decreased activity of the −1410 external deletion construct relative to position −1535; however, the sequences between positions −1535 and −1410 were not critical for developmental regulation. HCR contained both activating and repressing activities and resisted attempts to isolate separable segments responsible for each type of activity. In keeping with the close relationship between the repressing and activating activities of HCR was the inability of any of the mapping constructs to activate the promoter during growth in yeast-inducing conditions. Thus, the mechanisms of repression and activation appeared to be intertwined within this sequence. Activation conferred by HCR did not reach wild-type levels but was amplified by a distal region of the promoter that was not able to confer developmental expression on its own. The regions downstream of position −1042, in contrast, showed minimal activating function and appeared to be dispensable based on the independent functioning of HCR in the developmental regulation of a chimeric promoter.

The identities of the proteins that bound HCR from crude extracts strongly implicate chromatin structure in the activation of the *HWP1* gene. Nhp6 contains a single HMG box domain that is responsible for DNA binding (http://smart.embl-heidelberg.de) and belongs to the HMG1 subfamily of HMG proteins (9) that bind to DNA in either a sequence-specific or -nonspecific fashion (44). Nhp6 was found to specifically bind to the HCRa region in YE, HE, and STE under conditions of high stringency. Although both native Nhp6 and recombinant Nhp6 were selective for HCRa in competition assays using control DNA under conditions of high stringency, Nhp6 did not protect specific DNA sites in HCRa from DNase I cleavage as seen on urea-denaturing gels (data not shown). These findings are consistent with a high affinity of binding of Nhp6 to HCRa that is characteristic of this class of HMG proteins (44). Nhp6 was also present in extracts from 2-h hyphae, 2-h yeast, and stationary-phase cells, confirming its continued presence during hyphal growth beyond the 1-h time point used in the data reported herein (data not shown).

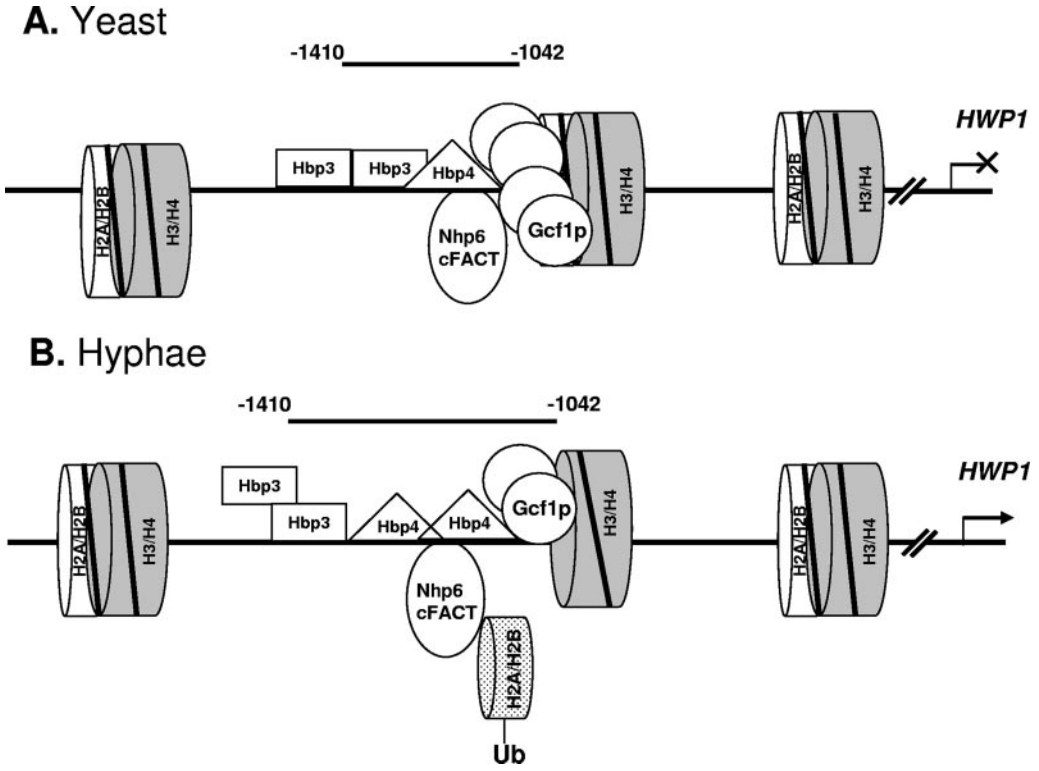

FIG. 8. Proposed model for the developmental regulation of the *HWP1* gene. (A) Under yeast growth conditions, tightly compacted DNA-histone octamers (white disks, H2A/H2B; gray disks, H3/H4) and relatively strong binding of Gcf1p (Hbp1) (circles) and Hbp3 (squares) to the HCR region inhibit occupation of DNA by activators. (B) Under germ tube-inducing conditions, a putative cFACT containing Nhp6 (oval) functions in facilitating the removal of ubiquitinized H2A and/or H2B (dotted disk) and relaxes DNA on nucleosomes, thereby permitting an enhancer (Hbp4) (triangles) to gain access to the promoter region to activate the *HWP1* gene. The location of HCR (positions −1410 to −1042) is indicated on the top of each model.

The identification of an HMG-like HCRa binding protein, Gcf1p, which has a domain showing weak similarity (30%) to a *P. polycephalum* protein nicknamed Glom because of its function in the compact condensation of mitochondrial DNA (36), provided further support for the influence of chromatin structure in *HWP1* promoter regulation. Gcf1p showed higher binding activity in yeast cultures than in hyphal cultures and appeared to show conformational changes between yeast and hyphal growth conditions. The increased presence of Gcf1p in yeast might reflect its contribution to repressing *HWP1* promoter activation in yeast (see below), although this function requires further investigation.

The identification of histones in HCRa binding is consistent with the relative ease of reconstitution of mononucleosomes in vitro with purified core histones and DNA fragments that range from about 150 bp to 250 bp in length (24). Also consistent with this, the 49th fraction prepared using heparin-Sepharose column chromatography and the 60% ammonium sulfate precipitation formed a complex with the 249-bp HCRa fragment on nondenaturing gels that turned out to contain two histones indicative of an H2A/H2B dimer (Table 3).

Potential interactions between H2A/H2B and Nhp6, as suggested by their coelution in the same column fraction (Fig. 3E), and the increased activity of Nhp6 in HE (Fig. 2) prompt a partial model for *HWP1* promoter activation based on the role of *S. cerevisiae* Nhp6 in chromatin reorganization and in transcriptional initiation and elongation (5, 13) (Fig. 8). Of particular interest is a transcription elongation factor called FACT (facilitates chromatin transcription), which restructures chromatin in the absence of ATP hydrolysis (34). In *S. cerevisiae*, the FACT complex consists of Spt16/Cdc68, Pob3, and Nhp6 and functions in histone degradation, the initiation of transcription (13, 25, 35, 45), and the promotion of TATA binding protein binding to a TATA box in chromatin both in vivo and in vitro (5). Proteins with 50 and 55% identities to *S. cerevisiae* Spt16 and Pob3 are present in the *C. albicans* SC5314 genome. In HeLa cells, FACT binds to nucleosomes following the monoubiquitination of lysine residue 120 of histone H2B and facilitates the removal of H2A/H2B and, ultimately, the separation of DNA from the nucleosome (32).

NHP6 mRNA was detected equally in both yeast and hyphal cells by reverse transcription-PCR (data not shown), arguing against increased *NHP6* expression being responsible for the enhanced activity of Nhp6 in gel mobility shifts using HE. Although the reasons for increased activity in hyphal extracts are unknown, one possibility is that preferred interactions with the H2A/H2B dimer in hyphae based on putative hypha-specific posttranslational modifications at their respective C termini would contribute to Nhp6's enhanced binding activity in HE if Nhp6 is indeed a subunit of a putative *C. albicans* FACT (cFACT) complex. cFACT-histone interactions may relax chromatin in the promoter region during activation. The pres-

ence and function of a cFACT complex are potentially fruitful areas of investigation for understanding *HWP1* promoter regulation.

Our characterization of HCRa binding proteins has provided insight into the complex nature of repressing and activating functions at the *HWP1* promoter that became evident from our GFP reporter studies. One possible scenario for the regulatory functions of these DNA binding proteins is that Gcf1p (Hbp1) and Hbp3, which show higher binding activities in YE, act as repressors of *HWP1* transcription, whereas Nhp6 (Hbp2) and Hbp4, which have increased activities in HE, act as activators. The lesser activities of Gcf1p and Hbp3 in HE and Nhp6 and Hbp4 in YE are suggestive of a model of competition between these proteins for binding to HCRa that is dependent on growth conditions to determine which HCRa binding factors are expressed in their activated forms at levels favoring successful binding to the promoter.

Further support for the idea that the *HWP1* promoter is regulated in a growth condition-dependent manner by repressing and/or activating factors at HCRa is shown by the observation that Hbp3 and Nhp6 (Hbp2) were found to bind near the 5′ end of HCRa between positions −1410 and −1289, whereas Gcf1p and Hbp4 formed protein-DNA complexes closer to the 3′ end between positions −1365 and −1162 (data not shown). It is possible that under yeast growth conditions, multimeric forms of Gcf1p interact with HCRa along with Hbp3, thereby impeding Nhp6 and Hbp4 from binding and imposing repression. In support of this model, we found that under germ tube-inducing conditions, Gcf1p appeared to be less multimerized, possibly as a result of conformational changes or loss or gain of posttranslational modifications, and Hbp3 showed reduced binding activity, potentially because of reduced expression. This shift in expression patterns would allow Nhp6 or Nhp6-interacting proteins and Hbp4 to gain access to HCR and enhance *HWP1* expression. Since the binding of Hbp3 and Nhp6 as well as that of Gcf1p and Hbp4 potentially overlap, competition for binding in HCRa that would be dependent on growth conditions would be expected to occur.

Several conclusions regarding the *HWP1* promoter are in agreement with those of Brown and coworkers, who studied the developmentally regulated *ALS3* gene. The spatial pattern of a critical region capable of conferring developmental regulation and a distal region that amplified the effect of this critical region was found for both promoters, although these elements were much closer to the coding region in the case of the *ALS3* promoter. The relationship between the distal and proximal regions in terms of the former enhancing the latter was verified by kinetic studies for both promoters, and the critical regions were both longer than would be predicted based on standard transcription factor binding motifs. Attempts to further delimit the critical regions, 150 bp for *ALS3* and 368 bp for *HWP1*, were not fruitful in either study. Subtle differences between the two promoters were also noted. The *HWP1* promoter appeared to activate GFP expression to higher levels, and the period of activation was extended well past the 1-h peak shown for the *ALS3* promoter.

For both the *ALS3* and *HWP1* promoters, the critical activating regions were notable for the paucity of morphogenetic transcription factor binding sites for known regulators such as Efg1, Tec1, Cph1, and Cph2. Consistent with its role in the activation of the *ALS3* promoter, as shown using a *bcr1*Δ/*bcr1*Δ mutant (30), Bcr1 also functioned in the activation of the *HWP1* promoter, although the *HWP1* promoter retained 37% activating activity relative to HB-12 in the *bcr1*Δ/*bcr1*Δ mutant background (not shown).

Activating regions from both promoters showed evidence of sites for repressor activity located in close proximity. Besides the potential for repression mediated by chromatin-condensing activities described above, strong evidence for the function of Nrg1 was found. A single binding site for Nrg1 was found in the critical activation regions of both the *ALS3* and *HWP1* promoters. Increased activation of both promoters (not shown for *HWP1*) was found in yeast growth conditions using *nrg1*Δ/*nrg1*Δ and *tup1*Δ/*tup1*Δ null mutants. Although Nrg1 was not among the four proteins identified from crude extracts of *C. albicans* that bound to HCRa, it may be one of the unidentified factors that was observed in gel mobility shift experiments. Overall, both studies supported the assertion that hypha-specific promoters are complex and are likely to be regulated by multiple factors.

ACKNOWLEDGMENTS

Support for this research was generously provided by the National Institute of Allergy and Infections Diseases (R01 AI46608). P. Sundstrom is a recipient of a Scholar Award from the Burroughs Wellcome Fund.

We thank Abraham L. Sonenshein and Ronald K. Taylor for providing helpful comments on the manuscript and Sarah Thompson, Michael D. Meeks, and Jennifer L. Snide for excellent technical assistance.

REFERENCES

1. **Abeyrathne, P. D., and R. N. Nazar.** 2000. Plasmid-enhanced strategy for PCR-mediated mutagenesis with difficult DNA templates. BioTechniques **29:**1172–1174.
2. **Ali, S. A., and A. Steinkasserer.** 1995. PCR-ligation-PCR mutagenesis: a protocol for creating gene fusions and mutations. BioTechniques **18:**746–750.
3. **Bahn, Y. S., J. Staab, and P. Sundstrom.** 2003. Increased high-affinity phosphodiesterase *PDE2* gene expression in germ tubes counteracts *CAP1*-dependent synthesis of cyclic AMP, limits hypha production and promotes virulence of *Candida albicans*. Mol. Microbiol. **50:**391–409.
4. **Bahn, Y. S., and P. Sundstrom.** 2001. *CAP1*, an adenylate cyclase-associated protein gene, regulates bud-hypha transitions, filamentous growth, and cyclic AMP levels and is required for virulence of *Candida albicans*. J. Bacteriol. **183:**3211–3223.
5. **Biswas, D., Y. Yu, M. Prall, T. Formosa, and D. J. Stillman.** 2005. The yeast FACT complex has a role in transcriptional initiation. Mol. Cell. Biol. **25:**5812–5822.
6. **Braun, B. R., and A. D. Johnson.** 1997. Control of filament formation in *Candida albicans* by the transcriptional repressor *TUP1*. Science **277:**105–109.
7. **Braun, B. R., and A. D. Johnson.** 2000. *TUP1*, CPH1, and *EFG1* make independent contributions to filamentation in *Candida albicans*. Genetics **155:**57–67.
8. **Brummel, M., and D. R. Soll.** 1982. The temporal regulation of protein synthesis during synchronous bud or mycelium formation in the dimorphic yeast *Candida albicans*. Dev. Biol. **89:**211–224.
9. **Bustin, M.** 2001. Chromatin unfolding and activation by HMGN(*) chromosomal proteins. Trends Biochem. Sci. **26:**431–437.
10. **Cohen, S. L., and B. T. Chait.** 1997. Mass spectrometry of whole proteins eluted from sodium dodecyl sulfate-polyacrylamide gel electrophoresis gels. Anal. Biochem. **247:**257–267.
11. **Costigan, C., D. Kolodrubetz, and M. Snyder.** 1994. *NHP6A* and *NHP6B*, which encode HMG1-like proteins, are candidates for downstream components of the yeast *SLT2* mitogen-activated protein kinase pathway. Mol. Cell. Biol. **14:**2391–2403.
12. **Fonzi, W. A., and M. Y. Irwin.** 1993. Isogenic strain construction and gene mapping in *Candida albicans*. Genetics **134:**717–728.
13. **Formosa, T., S. Ruone, M. D. Adams, A. E. Olsen, P. Eriksson, Y. Yu, A. R.**

Rhoades, P. D. Kaufman, and D. J. Stillman. 2002. Defects in *SPT16* or *POB3* (yFACT) in *Saccharomyces cerevisiae* cause dependence on the Hir/Hpc pathway: polymerase passage may degrade chromatin structure. Genetics **162:**1557–1571.
14. **Gillum, A. M., E. Y. H. Tsay, and D. R. Kirsch.** 1984. Isolation of the *Candida albicans* gene for orotidine-5′-phosphate decarboxylase by complementation of *S. cerevisiae* ura3 and *E. coli* pyrF mutations. Mol. Gen. Genet. **198:**179–182.
15. **Hornby, J. M., R. Dumitru, and K. W. Nickerson.** 2004. High phosphate (up to 600 mM) induces pseudohyphal development in five wild type *Candida albicans*. J. Microbiol. Methods **56:**119–124.
16. **Kadosh, D., and A. D. Johnson.** 2005. Induction of the *Candida albicans* filamentous growth program by relief of transcriptional repression: a genome-wide analysis. Mol. Biol. Cell **16:**2903–2912.
17. **Kim, S. I., C. Jourlin-Castelli, S. R. Wellington, and A. L. Sonenshein.** 2003. Mechanism of repression by *Bacillus subtilis* CcpC, a LysR family regulator. J. Mol. Biol. **334:**609–624.
18. **Kruppa, M., and D. Kolodrubetz.** 2001. Mutations in the yeast Nhp6 protein can differentially affect its *in vivo* functions. Biochem. Biophys. Res. Commun. **280:**1292–1299.
19. **Kumamoto, C. A., and M. D. Vinces.** 2005. Contributions of hyphae and hypha-co-regulated genes to *Candida albicans* virulence. Cell. Microbiol. **7:**1546–1554.
20. **Kurtz, M. B., M. W. Cortelyou, and D. R. Kirsch.** 1986. Integrative transformation of *Candida albicans*, using a cloned *Candida ADE2* gene. Mol. Cell. Biol. **6:**142–149.
21. **Kurzai, O., C. Schmitt, E. Brocker, M. Frosch, and A. Kolb-Maurer.** 2005. Polymorphism of *Candida albicans* is a major factor in the interaction with human dendritic cells. Int. J. Med. Microbiol. **295:**121–127.
22. **Laemmli, U. K.** 1970. Cleavage of structural proteins during the assembly of the head of bacteriophage T4. Nature **227:**680–685.
23. **Lane, S., S. Zhou, T. Pan, Q. Dai, and H. Liu.** 2001. The basic helix-loop-helix transcription factor Cph2 regulates hyphal development in *Candida albicans* partly via *TEC1*. Mol. Cell. Biol. **21:**6418–6428.
24. **Lusser, A., and J. T. Kadonaga.** 2004. Strategies for the reconstitution of chromatin. Nat. Methods **1:**19–26.
25. **Malone, E. A., C. D. Clark, A. Chiang, and F. Winston.** 1991. Mutations in *SPT16*/*CDC68* suppress *cis*- and *trans*-acting mutations that affect promoter function in *Saccharomyces cerevisiae*. Mol. Cell. Biol. **11:**5710–5717.
26. **Mao, X., F. Cao, X. Nie, H. Liu, and J. Chen.** 2006. The Swi/Snf chromatin remodeling complex is essential for hyphal development in *Candida albicans*. **580:**2615–2622.
27. **Murad, A. M., P. Leng, M. Straffon, J. Wishart, S. Macaskill, D. MacCallum, N. Schnell, D. Talibi, D. Marechal, F. Tekaia, C. d'Enfert, C. Gaillardin, F. C. Odds, and A. J. Brown.** 2001. NRG1 represses yeast-hypha morphogenesis and hypha-specific gene expression in Candida albicans. EMBO J. **20:**4742–4752.
28. **Nantel, A., D. Dignard, C. Bachewich, D. Harcus, A. Marcil, A. P. Bouin, C. W. Sensen, H. Hogues, M. van het Hoog, P. Gordon, T. Rigby, F. Benoit, D. C. Tessier, D. Y. Thomas, and M. Whiteway.** 2002. Transcription profiling of *Candida albicans* cells undergoing the yeast-to-hyphal transition. Mol. Biol. Cell **13:**3452–3465.
29. **Nelson, D. A., W. R. Beltz, and R. L. Rill.** 1977. Chromatin subunits from baker's yeast: isolation and partial characterization. Proc. Natl. Acad. Sci. USA **74:**1343–1347.
30. **Nobile, C. J., and A. P. Mitchell.** 2005. Regulation of cell-surface genes and biofilm formation by the *C. albicans* transcription factor Bcr1p. Curr. Biol. **15:**1150–1155.
31. **Olson, M. V., J. E. Dutchik, M. Y. Graham, G. M. Brodeur, C. Helms, M. Frank, M. MacCollin, R. Scheinman, and T. Frank.** 1986. Random-clone strategy for genomic restriction mapping in yeast. Proc. Natl. Acad. Sci. USA **83:**7826–7830.
32. **Pavri, R., B. Zhu, G. Li, P. Trojer, S. Mandal, A. Shilatifard, and D. Reinberg.** 2006. Histone H2B monoubiquitination functions cooperatively with FACT to regulate elongation by RNA polymerase II. Cell **125:**703–717.
33. **Raman, S. B., M. H. Nguyen, Z. Zhang, S. Cheng, H. Y. Jia, N. Weisner, K. Iczkowski, and C. J. Clancy.** 2006. *Candida albicans SET1* encodes a histone 3 lysine 4 methyltransferase that contributes to the pathogenesis of invasive candidiasis. **60:**697–709.
34. **Rhoades, A. R., S. Ruone, and T. Formosa.** 2004. Structural features of nucleosomes reorganized by yeast FACT and its HMG box component, Nhp6. Mol. Cell. Biol. **24:**3907–3917.
35. **Rowley, A., R. A. Singer, and G. C. Johnston.** 1991. *CDC68*, a yeast gene that affects regulation of cell proliferation and transcription, encodes a protein with a highly acidic carboxyl terminus. Mol. Cell. Biol. **11:**5718–5726.
36. **Sasaki, N., H. Kuroiwa, C. Nishitani, H. Takano, T. Higashiyama, T. Kobayashi, Y. Shirai, A. Sakai, S. Kawano, K. Murakami-Murofushi, and T. Kuroiwa.** 2003. Glom is a novel mitochondrial DNA packaging protein in *Physarum polycephalum* and causes intense chromatin condensation without suppressing DNA functions. Mol. Biol. Cell **14:**4758–4769.
37. **Schweizer, A., S. Rupp, B. N. Taylor, M. Rollinghoff, and K. Schroppel.** 2000. The TEA/ATTS transcription factor CaTec1p regulates hyphal development and virulence in *Candida albicans*. Mol. Microbiol. **38:**435–445.
38. **Snide, J. L., and P. Sundstrom.** 2006. A characterization of *HWP1* promoter activation in pseudohyphal cells in *Candida albicans*, abstr. C192, p. 103. Abstr. 8th ASM Conf. *Candida* Candidiasis. American Society for Microbiology, Washington, DC.
39. **Staab, J. F., Y.-S. Bahn, and P. Sundstrom.** 2003. Integrative, multifunctional plasmids for hypha-specific or constitutive expression of green fluorescent protein in *Candida albicans*. Microbiology **149:**2977–2986.
40. **Staab, J. F., S. D. Bradway, P. L. Fidel, and P. Sundstrom.** 1999. Adhesive and mammalian transglutaminase substrate properties of *Candida albicans* Hwp1. Science **283:**1535–1538.
41. **Staab, J. F., C. A. Ferrer, and P. Sundstrom.** 1996. Developmental expression of a tandemly repeated, proline- and glutamine-rich amino acid motif on hyphal surfaces on *Candida albicans*. J. Biol. Chem. **271:**6298–6305.
42. **Stoldt, V. R., A. Sonneborn, C. E. Leuker, and J. F. Ernst.** 1997. Efg1p, an essential regulator of morphogenesis of the human pathogen *Candida albicans*, is a member of a conserved class of bHLH proteins regulating morphogenetic processes in fungi. EMBO J. **16:**1982–1991.
43. **Sudbery, P., N. Gow, and J. Berman.** 2004. The distinct morphogenic states of *Candida albicans*. Trends Microbiol. **12:**317–324.
44. **Thomas, J. O.** 2001. HMG1 and 2: architectural DNA-binding proteins. Biochem. Soc. Trans. **29:**395–401.
45. **Yu, Y., P. Eriksson, and D. J. Stillman.** 2000. Architectural transcription factors and the SAGA complex function in parallel pathways to activate transcription. Mol. Cell. Biol. **20:**2350–2357.
46. **Yuh, C. H., A. Ransick, P. Martinez, R. J. Britten, and E. H. Davidson.** 1994. Complexity and organization of DNA-protein interactions in the 5′-regulatory region of an endoderm-specific marker gene in the sea urchin embryo. Mech. Dev. **47:**165–186.